Utrecht University

Department of Mathematics

Sharp Asymptotics and Simulations for Probabilistic Cellular Automata

Reinier Nederstigt

A thesis presented in partial fulfilment of the requirements for the degrees of

Bachelor in Mathematics and Bachelor in Physics

Supervisor:

Dr. C. Spitoni Supervisor
Department of Mathematics, Utrecht University

June 13, 2018

Abstract

In this thesis, the problem of metastability for a finite volume Probabilistic Cellular Automata (PCA) in a small external field in the low temperature limit is studied, corresponding to the parallel implementation of the Ising model in a heat bath. In particular, the exit time of the metastable state (the configuration with al pluses), i.e. the time spent nucleating the stable state (the configuration with al pluses) triggered by the formation of a critical droplet, is of interest. The main result of the thesis is the sharp estimate on the mean of the exit times, which is an exponential function of the inverse temperature β times a prefactor that does not scale with β. Additionally finite temperature Markov chain Monte Carlo (MCMC) simulations are performed on PCA that correspond to ferromagnetic and anti-ferromagnetic stochastic lattice spin models.

Contents

1 Introduction

Metastability is a phenomena common in nature when a physical system is close to a first order phase transition. It is often characterised by the phenomenological property that a system can persist for a long length of time in a phase different from the equilibrium predicted by thermodynamics. Well known examples of metastable systems are super-cooled liquids and magnetic hysteresis, in which the latter is the result of an external magnetic field applied to a ferromagnet such that the dipole moments will spontaneously self align. This alignment is retained even after the external field is removed, *magnetising* the material. A rigorous mathematical description of this behaviour was only recently formulated, pioneered by the paper [1], and experienced substantial progress since.

A natural approach towards analysing the metastable behaviour is that of Markov chains, or Markov processes, describing the discrete time evolution of a statistical mechanical system. Then, by considering metastable states as local minima of the energy landscape, the problem is reduced to the computation of the minimal energy barrier, called the *communication energy*, in which a path connecting the metastable and stable state needs to overcome. This leads to a minimax problem over all possible paths connecting the two states, which are generally quite complicated, but becomes particularly difficult when the dynamics are of a parallel nature. When allowing for simultaneous updates to the systems states, the continuity constrains on the structure of the trajectories in the configuration space are broken, i.e. the communication energy cannot merely be stated in terms of the energy difference but has to account for all possible transitions in the configuration space.

We shall study the metastability problem in the framework of *Probabilistic Cellular Automata* (PCA). PCA are discrete time Markov chains with a stochastic parallel updating rule on a lattice with finite single-cell states, allowing them to be studied with the theory of Markov processes. Moreover, we particularly study PCA that belong to the family of reversible PCA with a local updating rule, in the sense that it depends only on the value of the variables in a finite subset fo the lattice containing the site itself, as introduced by [8]. We shall refer to an update rule that is dependent on the value of the site itself as *self-interacting*. More notably, the model studied in [7] is a PCA without self-interaction, which can be considered the parallel implementation of the Ising model in a heat bath. In this context, the single-cell states are given by either -1 or $+1$, the metastable state by $-\underline{1}$ (the configuration with all minuses), and the stable state $+\underline{1}$ (the configuration with all pluses). Therefore, it can be seen as an example of the process of magnetic hysteresis, which will be a recurrent theme. Furthermore, it is proven that the PCA exhibit different metastable behaviour in comparison to a sequential implementation of the heat bath dynamics, i.e. starting from the metastable phase $-\underline{1}$ the system visits with probability one a chessboard-like phase before reaching the stable phase $+\underline{1}$.

In this thesis, however, we will rigorously investigate the metastability behaviour of a reversible PCA with a self-interaction, reproducing the sharp estimate on the asymptotics for the mean nucleation time of the stable state in [10], with a novel proof pertaining the lower bound. Moreover, a class of reversible PCA with a parameter tuning between self- and non self-interaction is analysed on the basis of heuristic and numerical grounds, reproducing and expanding on the numerical results in [5]. In both cases, controlling for the strength of the self-interaction, the local updating rule is allowed to behave as some majority rule on the neighbourhood of the site in question, varying the role played by the intermediate chessboard-like phase. Hence, these PCA present non trivial metastable behaviour, which makes this class of models physically very interesting.

Difficulties in studying these PCA arises due to the existence of many local minima in which the system can be trapped, i.e. the zero temperature dynamics has a large variety of fixed points and cyclic pairs. For example in the case of no self-interaction, chessboard-like phases will be stable, only flip-flopping between parity. The solution is provided through the application of a potential theoretic approach to our model, by remarking that any reversible irreducible Markov chain on a finite state space is the random walk associated with some electrical network. The notion of a *capacity* on the electrical network can then be exploited to define the metastable states in terms of capacities such that the precise asymptotics for the mean exit time from a metastable state follows via general theorems. Hence, the problem is reduced to obtaining sharp

upper and lower bounds on the capacities. In fact, the upper bound is derived from the Dirichlet variational principle, which represents a capacity as an *infimum* over a class of test functions. Furthermore, lower bounds can be derived from a reduced electrical network and the monotonicity of the Dirichlet form.

However, three model dependent results, proven in [6] are needed for the application of the potential theoretic approach, namely

(i) the solution for the global variational problem for all paths connecting the metastable and stable state, i.e. the computation of the communication energy,

(ii) a sort of recurrence property stating that, starting from each configuration different from the metastable and stable state, it is possible to reach a configuration at lower energy, following a path with an energy cost strictly smaller than the communication energy, and

(iii) the determination of a particular set of configurations, i.e. the *critical configurations* for the transition from metastable to stable state and the neighbour of this set. This set of critical configurations is typically visited by the system during its transition from the metastable to the stable state, and plays the role of the saddle configurations in the energy landscape.

Here, points (i) and (ii) are needed to prove that there are only two configurations belonging to the metastable set, i.e. $-\underline{1}$ the proper metastable state, and $+\underline{1}$ the stable state, according to Definition 2.24. Moreover, the recurrence property (ii) prevents the presence of *deep wells* in the energy landscape, where the system can be trapped for a huge length of time. Lastly, points (i) and (iii) are used in calculating the capacity between $-\underline{1}$ and $+\underline{1}$, and, in particular, the prefactor of the nucleation time is directly related to the cardinality of the set of saddles.

The outline of this thesis is as follows. In Section 2.1 a formal mathematical introduction into discrete space discrete Markov chains will be presented, on which will be expanded. An equilibrium potential will be associated with the Markov chain in Section 2.2, in particular a potential theoretical approach to metastability is reviewed. Moreover, a definition of the capacities via a variational problem is given in Section 2.2.1. Then, in Section 2.3 a general theorem is presented on the mean exit time of a metastable state, detailing the metastable behaviour of the Markov chain and formally defining the notion of metastability in terms of capacities.

In Section 3 the main theorem will be stated, based on useful definitions introduced on the energy landscape in the beginning of the section. The remaining part of the section is, in large part, devoted on the sharp estimation of the capacity between the metastable states, by obtaining appropiate upper and lower bounds. Proving the main result of this thesis.

Lastly, Section 4 details the use of Markov chain Monte Carlo methods for researching certain aspects of the metastable behaviour of the PCA. More generally, this section aims to show the benefit of using numeric results in combination with rigorous analysis. Four numerical experiments are performed, investigating the finite temperature behaviour of the PCA with self-interaction, the multiple metastability scenario's for a ferromagnetic kernel and its dynamic interactions, and lastly the anti-ferromagnetic case is considered.

2 Markov processes

The following section will contain a short review on the theory of Markov process, with emphasis on discrete space discrete time Markov chains, the potential theoretic approach and their application on PCA. It will closely follow the lecture notes of A. Bovier in [2] and A. Gaudillière in [9], given that their works provide the reader with a clear and systematic introduction to the subject of a potential theoretic approach.

2.1 Definitions

Let us first introduce the mathematical definition of Markov processes.

Definition 2.1. *A stochastic process $\chi = \{X_t\}_{t\in I}$, with $X_t \in \mathcal{S}$ is called a **Markov process** with ordered index set I and state space $\mathcal{S}$, if for any collection $t_1 < ... < t_n < t \in I$, and*

$$\mathbb{P}[X_t \in \mathcal{A} \mid X_{t_n} = x_n, ..., X_{t_1} = x_1] = \mathbb{P}[X_t \in \mathcal{A} \mid X_{t_n} = x_n] \tag{2.1}$$

for any Borel set $\mathcal{A} \in \mathcal{B}(\mathcal{S})$.

Put into words, a Markov process is a stochastic process with the memoryless property, i.e. the transition to future states of the process only depend on the current state, and not on the history of the process. We will refer to this as the *Markov property*. Since the index set I is an ordered set, in particular either $\mathbb{N}$ or $\mathbb{R}$, we will respectively distinguish between a discrete time *Markov chain* and a continuous time Markov process. Additionally, $\mathcal{S}$ may be finite, countable, or even uncountable.

Henceforth, we will only consider the case of discrete time Markov chains with a discrete and finite state space $\mathcal{S}$. In doing so, we introduce a short hand notation for the family of probability measures p on $\mathcal{S} \times \mathcal{B}(\mathcal{S})$

$$p(s, t, x, \mathcal{A}) := \mathbb{P}[X_t \in \mathcal{A} \mid X_s = x], \tag{2.2}$$

for any Borel set $\mathcal{A} \in \mathcal{B}(\mathcal{S})$. Note that by (2.1), the law of the stochastic process is uniquely determined by $p(s, t, x, \cdot)$. Moreover, we will only be concerned with *time-homogeneous* Markov processes, i.e., $p(s, t, x, \cdot)$ is a function of $t - s$ only, and let

$$p(s, t, x, \cdot) := p_{t-s}(x, \cdot). \tag{2.3}$$

Lastly, since we only consider the case of discrete time Markov chains and discrete space, (2.1) implies that the *transition matrix* P is fully determined by the *one-step transition kernel*,

$$p(x, \cdot) \coloneqq p_1(x, \cdot). \tag{2.4}$$

It will be convenient to denote by $\mathbb{P}_x$ the law of the Markov chain conditioned on $X_0 = x$, and define a 'generator' of the discrete time Markov chain as

$$\mathcal{L} := 1 - P. \tag{2.5}$$

Within this setting, we will think of P and $\mathcal{L}$ as operators acting on functions f and measures ρ on $\mathcal{S}$, via

$$\begin{aligned} (Pf)(x) &:= \sum_{y\in\mathcal{S}} p(x, y)f(y), \text{ and} \\ (\rho P)(x) &:= \sum_{x\in\mathcal{S}} \rho(x)p(x, y). \end{aligned} \tag{2.6}$$

Next, we will introduce a few properties of Markov chains, which will prove to be essential.

Definition 2.2. *Let χ denote a Markov chain with state space $\mathcal{S}$, then for any set $D \subset \mathcal{S}$, we define the **first hitting time** τ_D for χ as*

$$\tau_D := \inf \{t > 0 \mid X_t \in D\}. \tag{2.7}$$

Note that τ_D is a *stopping time*, i.e., the random variable τ_D depends only on the evolution of the chain χ up to time t, which we will refer to as the *strong Markov property.*

Definition 2.3. *A Markov chain χ with state space $\mathcal{S}$ is called **irreducible** if for any $x, y \in \mathcal{S}$, there exists a $t < \infty$ such that $p_t(x, y) > 0$.*

The notion of irreducibility can be thought of in terms of equivalence relations, in which two states $x, y \in \mathcal{S}$ belong to the same equivalence class if there is a non-zero transition probability between them. Then a Markov chain is set to be irreducible if and only if it has just one communication class.

Definition 2.4. *A Markov chain χ with state space $\mathcal{S}$ is called **recurrent** if it is irreducible and $\mathbb{P}_x[\tau_x < \infty] = 1$ for all $x \in \mathcal{S}$. Moreover, it is called **positive recurrent** if $\mathbb{E}_x \tau_x < \infty$ for all $x \in \mathcal{S}$.*

That is, given that a recurrent Markov chain starts at $x \in \mathcal{S}$, it will return to x in a finite amount of time with probability 1. Alternatively, if a Markov chain starting at $x \in \mathcal{S}$ is recurrent, it implies that it has no *deep wells* in which the chain can be trapped, preventing a return to x. Moreover, note that positive recurrency does not imply recurrency, though the following theorem does holds.

Theorem 2.5. *Let χ denote an irreducible Markov chain with finite state space $\mathcal{S}$, then χ is positive recurrent.*

Proof. See [11].

□

This is the first of three useful properties obtained for irreducible Markov chains with finite state space. The second can be found by defining the following probability measure.

Definition 2.6. *Let χ denote a Markov chain with state space $\mathcal{S}$ and transition matrix P. Then a probability measure μ on $\mathcal{S}$ is called a **stationary distribution** (or **invariant measure**) of χ if and only if $\mu P = P$, i.e.*

$$\sum_{x \in \mathcal{S}} \mu(x) p(x, y) = \mu(y) \qquad \forall y \in \mathcal{S}. \tag{2.8}$$

Note that (2.8) is equivalent to setting,

$$\mu \mathcal{L} = 0. \tag{2.9}$$

The following theorem can now be formulated.

Theorem 2.7. *Let χ denote an irreducible Markov chain with finite state space $\mathcal{S}$, then χ has an unique stationary distribution μ.*

Proof. See [11].

□

Hence, the second property ensures the existence of an unique stationary distribution. Lastly, we introduce the notion of time-reversibility, that is when a reverse-time Markov chain has the same stationary distribution as the forward-time stationary Markov chain. More formally,

Definition 2.8. *Let χ denote a Markov chain with transition matrix P. Then a non-zero probability measure π on $\mathcal{S}$ is called **reversible** with respect to P if and only if it satisfies the **detailed balance equations**, i.e.*

$$\pi(x) p(x, y) = \pi(y) p(y, x) \qquad \forall x, y \in \mathcal{S}. \tag{2.10}$$

The third property can be summarised in the following proposition.

Proposition 2.9. *Let χ denote an irreducible Markov chain with finite state space $\mathcal{S}$ and transition matrix P. If there exists a probability solution π to detailed balance equations, then χ is reversible and the solution π is the unique stationary distribution μ.*

Proof. Note that since χ is irreducible, has a finite state space $\mathcal{S}$ and π satisfies the set of time-reversibility equations, it follows that χ is reversible and there exists a unique stationary distribution μ.

$$\begin{aligned}\pi(x)p(x,y) = \pi(y)p(y,x) \quad \Leftrightarrow \quad \sum_x \pi(x)p(x,y) &= \sum_x \pi(y)p(y,x) \\ &= \pi(y)\sum_x p(y,x) \\ &= \pi(y) \times 1 \\ &= \pi(y)\end{aligned}$$

Hence, π is a stationary distribution of χ. Thus $\pi = \mu$.

□

Thus, considering an irreducible Markov chain with finite space state, one only needs to confirm that some distribution μ indeed satisfies the detailed balance equations to proof that, not only is the chain reversible, but also the distribution μ is the unique stationary distribution, implying that if a reversible measure exists it is unique.

2.2 A Potential Theoretic Approach

We will now focus on the connections between potential theory and Markov processes. To this end, we will only consider the case of discrete state space and discrete time. Let therefore denote χ a time-homogeneous Markov chain, i.e. set $p_1(x,y) = p(x,y)$. Moreover, we assume that χ is irreducible, reversible and has a finite state space $\mathcal{S}$. Then, by Proposition 2.9, this implies the existence of a unique time reversible stationary distribution μ.

The potential theoretical approach starts by identifying a probabilistic object that behaves as an equilibrium potential, which will be our starting point. Given two non-empty disjoint subsets $A, D \subset \mathcal{S}$ and $x \in \mathcal{S}$, the probability

$$\mathbb{P}_x[\tau_A < \tau_D], \tag{2.11}$$

i.e. the probability when starting in x, hitting A before D, is indeed a candidate for representing a potential and will therefore be instrumental in developing a potential theoretic approach for the analysis of metastable systems. The first task we thus face ourselves with is computing such probabilities.

Note that if $x \in \mathcal{S} \setminus (A \cup D)$, there are three possible scenario's to consider, i.e. either the first step always leads to $y \in D$, and the event $\{\tau_A < \tau_D\}$ does not occur, or to $y \in A$, in which case the event does occur, or lastly to $y \in \mathcal{S} \setminus (A \cup D)$, in which case the event occurs with probability $\mathbb{P}_y[\tau_A < \tau_D]$. Thus

$$\mathbb{P}_x[\tau_A < \tau_D] = \sum_{y \in A} p(x,y) + \sum_{y \in \mathcal{S}\setminus(A\cup D)} p(x,y)\mathbb{P}_y[\tau_A < \tau_D] \tag{2.12}$$

for all $x \in \mathcal{S} \setminus (A \cup D)$. Due to the reasoning, we will call equations of these kind *forward* equations. It will be convenient to introduce the function $h_{A,D}$ such that

$$h_{A,D}(x) := \begin{cases} \mathbb{P}_x[\tau_A < \tau_D], & \text{if } x \in \mathcal{S} \setminus (A \cup D) \\ 1, & \text{if } x \in A \\ 0, & \text{if } x \in D \end{cases} \tag{2.13}$$

Than (2.12) implies that $\mathcal{L}h_{A,D} = 0$ for all $x \in \mathcal{S} \setminus (A \cup D)$, i.e.

$$h_{A,D}(x) = \sum_{y \in \mathcal{S}} p(x,y)h_{A,D}(y). \tag{2.14}$$

Therefore, the function $h_{A,D}$ can be seen as the solution of the homogeneous *Dirichlet problem* represented by

$$\begin{aligned}(\mathcal{L}h_{A,D})(x) &= 0, \quad x \in \mathcal{S} \setminus (A \cup D),\\ h_{A,D}(x) &= 1, \quad x \in A,\\ h_{A,D}(x) &= 0, \quad x \in D.\end{aligned} \tag{2.15}$$

If we can prove that this problem has a unique solution, then the problem of computing the probabilities $\mathbb{P}_x[\tau_A < \tau_D]$ is reduced to a problem of linear algebra.

Proposition 2.10. *Let X denote an irreducible Markov chain with finite state space $\mathcal{S}$, and let $A, D \subset \mathcal{S}$ be two non-empty disjoint subsets. Then the boundary value problem (2.15) has a unique solution.*

Proof. See [9].

□

Since the solution is unique, we conclude the following:

Definition 2.11. *The function $h_{A,D}$ is called the **equilibrium potential** of the capacitor A, D.*

In order to continue we need to know what happens when $x \in A$ or $x \in D$, using the same arguments leading to (2.12), but now for $x \in \mathcal{S}$, together with our definition of $h_{A,D}$ we obtain the forward equation

$$\mathbb{P}_x[\tau_A < \tau_D] = \sum_{y \in A} p(x,y) + \sum_{y \in \mathcal{S}\setminus(A\cup D)} p(x,y)\mathbb{P}_y[\tau_A < \tau_D] = \sum_{y \in \mathcal{S}} p(x,y) h_{A,D}(y) \tag{2.16}$$

Consequently, it will be convenient to define the function $e_{A,D}$ as

$$e_{A,D}(x) := -(\mathcal{L}h_{A,D})(x). \tag{2.17}$$

Then

$$\mathbb{P}_x[\tau_A < \tau_D] = \begin{cases} h_{A,D}(x), & \text{if } x \in \mathcal{S} \setminus (A \cup D)\\ 1 - e_{A,D}(x), & \text{if } x \in A\\ e_{A,D}(x), & \text{if } x \in D \end{cases} \tag{2.18}$$

Therefore, we again conclude the following:

Definition 2.12. *The function $e_{A,D}$ is called the **escape probability** from A to D.*

Let us now consider the strength of the *probability flow* escaping from A to D.

Definition 2.13. *Given two non-empty disjoined subsets $A, D \subset \mathcal{S}$, the **capacity** of the capacitor A,D is defined as*

$$CAP(A,D) := \sum_{x \in D} \mu(x) e_{A,D}(x). \tag{2.19}$$

2.2.1 The Dirichlet Form

Although it is closely related to the equilibrium potential $h_{A,D}$ we are not interested in the definition of the capacity in terms of escape probabilities $e_{A,D}$. The introduction of the Dirichlet form allows for the definition to be rewritten to a surprisingly useful variational form, the Dirichlet principle.

Definition 2.14. *For any $h : \mathcal{S} \to \mathbb{R}$, define the **Dirichlet form** $\mathfrak{C}$ associated to the Markov process with generator $\mathcal{L}$ as*

$$\mathfrak{C}(h) := \sum_{x \in \mathcal{S}} \mu(x) h_{A,D}(x)(\mathcal{L}h_{A,D})(x) = \frac{1}{2} \sum_{x,y \in \mathcal{S}} \mu(x) p(x,y)[h(x) - h(y)]^2. \tag{2.20}$$

Hence,

Proposition 2.15. *The capacity can be represented in terms of the Dirichlet form.*

Proof. Since $\mu\mathcal{L} = 0$ and the properties of $h_{A,D}$ it follows that

$$\begin{aligned} CAP(A,D) &= \sum_{x\in D} \mu(x) e_{A,D}(x) \\ &= \sum_{x\in\mathcal{S}} \mu(x)(1-h_{A,D}(x))(-\mathcal{L}h_{A,D})(x) \\ &= \sum_{x\in\mathcal{S}} \mu(x)h_{A,D}(x)(\mathcal{L}h_{A,D})(x) - \sum_{x\in\mathcal{S}} (\mu\mathcal{L})(x)h_{A,D}(x) \\ &= \sum_{x\in\mathcal{S}} \mu(x)h_{A,D}(x)(\mathcal{L}h_{A,D})(x) \\ &= \mathfrak{C}(h_{A,D}) \end{aligned}$$

□

Furthermore,

Theorem 2.16 (**Dirichlet principle**). *Given two non-empty disjoined subsets $A, D \subset \mathcal{S}$,*

$$CAP(A,D) = \min_{\substack{h:\mathcal{S}\to[0,1] \\ h|_A:=1, h|_D:=0}} \mathfrak{C}(h) \tag{2.21}$$

Moreover, the variational problem (2.21) has a unique minimiser that is given by the equilibrium potential $h_{A,D}$.

Proof. Differentiating $\mathfrak{C}(h)$ with respect to $h(x)$ for $x \in \mathcal{S} \setminus (A \cup D)$ yields

$$\frac{\partial\mathfrak{C}(h)}{\partial h(x)} = 2(\mu\mathcal{L})(x)h(x).$$

If h minimises $\mathfrak{C}$, it must hold that $(\mathcal{L}h)(x) = 0$. And since we have already proven that the boundary value problem (2.15) has a unique solution, namely the equilibrium potential $h_{A,D}$, this finishes the proof.

□

From the variational problem (2.21) it follows that the capacity is a *symmetric* function of the sets A and B. Moreover, it allows the estimation of an an *upper bound* for the capacity by inserting a test function h into the Dirichlet form.

2.2.2 Electrical Networks

In order to display the relation between potential theory and that of Markov chains more explicitly, and even further exploit this relation, we shall briefly consider electrical networks and the notion of conductivity on these networks.

Definition 2.17. *An **electrical network** is a pair $(\mathcal{S}, c)$ with $\mathcal{S}$ a countable set and c a real valued non-negative symmetric function on $\mathcal{S}\times\mathcal{S}$, such that*

$$\mu(x) := \sum_{y\in\mathcal{S}} c(x,y) < +\infty \tag{2.22}$$

for all $x \in \mathcal{S}$, and such that for all distinct $x, y \in \mathcal{S}$, there exist $x = z_1, z_2, ..., z_n = y$ in $\mathcal{S}$ with

$$c(z_k, z_{k+1}) > 0 \tag{2.23}$$

*for all $k \in \{1, 2, ..., n-1\}$. We will refer to **nodes** the elements of $\mathcal{S}$, and say that two nodes x and y are **connected** when $c(x,y) > 0$, and **edges** as elements of Ω, defined as the set of ordered pairs of connected nodes*

$$\Omega := \{(x,y) \in \mathcal{S}\times\mathcal{S} \mid c(x,y) > 0\}. \tag{2.24}$$

*Therefore, we shall refer to $c(x,y)$ as the **conductance** between x and y.*

Remark 2.18. Note that any reversible irreducible Markov chain χ with finite state space $\mathcal{S}$ is the random walk associated with some electrical network $(\mathcal{S}, c)$, by

$$c(x, y) = \mu(x)p(x, y). \tag{2.25}$$

this association illustrates most clearly the fundamental relation between the theory of Markov chains and *potential theory.*

We can now identify the energy dissipated per time unit in a finite electrical network $(\mathcal{S}, c)$ by a potential h is in terms of the Dirichlet from by

$$\mathfrak{C}(h) := \frac{1}{2} \sum_{(x,y)\in\Omega} c(x, y)[h(x) - h(y)]^2. \tag{2.26}$$

Which suggests the following:

Definition 2.19. *Given two non-empty disjoined subsets A and D of a finite network $(\mathcal{S}, c)$, the* ***effective conductance*** *between A and D is defined as*

$$C(A, D) := \mathfrak{C}(h_{A,D}) \tag{2.27}$$

with obvious notation.

And as a consequence we have,

$$CAP(A, D) = \mathfrak{C}(h_{A,D}) = C(A, D). \tag{2.28}$$

Corollary 2.20. *Capacity and effective conductance coincide.*

This corollary leads directly to the following theorem:

Theorem 2.21 (**Rayleigh's monotonicity law**)**.** *If $c_1 \leq c_2$ are such that $(\mathcal{S}, c_1)$ and $(\mathcal{S}, c_2)$ are two finite electrical networks, then, given two non-empty disjoined subsets $A, D \subset \mathcal{S}$,*

$$CAP(A, D, c_1) \leq CAP(A, D, c_2), \tag{2.29}$$

with obvious notation.

Hence, if $\tilde{c} \leq c$ are such that $(\mathcal{S}, \tilde{c})$ is a *reduced* electrical network of $(\mathcal{S}, c)$, we can obtain a *lower bound* for the capacity. However, the drawback of this method is that it requires an estimation of the equilibrium potential $h_{A,D}$.

2.2.3 Renewal Equations

Up until this point, we have not yet addressed the fact that a way of computing of the equilibrium potential is still missing. Luckily, a very useful upper bound, i.e. the *renewal bound* can be found using a simple argument. First, let $A, D \subset \mathcal{S}$ be two non-empty disjoined subsets, such that D is just a point $x \in \mathcal{S}$, then by definition (2.13) it follows that

$$\mathbb{P}_x[\tau_A < \tau_x] = \frac{1}{\mu(x)} CAP(A, x). \tag{2.30}$$

This quantity denotes the probability that a process starting in a point x will go to A, without returning to x, and is therefore referred to as a *escape probability.* Now consider again a process starting in a point x, then the event $\{\tau_A < \tau_D\}$ can be realised in one of two ways, either by going to straight A without returning to x, or by returning to x without visiting A or D. Since, once the process returns to x, it can again realise the event $\{\tau_A < \tau_D\}$ in the same way as before, 'renewing' the process. Therefore, we can make the following observation.

Proposition 2.22. *Let $A, D \subset \mathcal{S}$ be two non-empty disjoined subsets, and $x \in \mathcal{S} \setminus (A \cup D)$, then*

$$\mathbb{P}_x[\tau_A < \tau_D] = h_{A,D}(x) \leq \frac{CAP(x,A)}{CAP(x,D)} \tag{2.31}$$

Proof. Using the Markov property to separate the joint probability results in,

$$\begin{aligned}\mathbb{P}_x[\tau_A < \tau_D] &= \mathbb{P}_x[\tau_A < \tau_{D\cup x}] + \mathbb{P}_x[\tau_x < \tau_{A\cup D} \cap \tau_A < \tau_D] \\ &= \mathbb{P}_x[\tau_A < \tau_{D\cup x}] + \mathbb{P}_x[\tau_x < \tau_{A\cup D}]\ \mathbb{P}_x[\tau_A < \tau_D]\end{aligned} \tag{2.32}$$

For obvious reasons (2.32) is called a *renewal* equation. Solving the renewal equation for $\mathbb{P}_x[\tau_A < \tau_D]$ yields,

$$\mathbb{P}_x[\tau_A < \tau_D] = \frac{\mathbb{P}_x[\tau_A < \tau_{D\cup x}]}{1 - \mathbb{P}_x[\tau_x < \tau_{A\cup D}]} = \frac{\mathbb{P}_x[\tau_A < \tau_{D\cup x}]}{\mathbb{P}_x[\tau_{A\cup D} < \tau_x]} \leq \frac{\mathbb{P}_x[\tau_A < \tau_x]}{\mathbb{P}_x[\tau_D < \tau_x]} = \frac{CAP(x,A)}{CAP(x,D)}.$$

□

Of course the renewal bound is only useful if it is smaller than 1. We now have demonstrated that the computation of the equilibrium potential can be reduced to that of the capacities, which will proof useful for our purposes.

2.2.4 Mean Hitting Times

Next, we will derive formulas for the mean values of the hitting times τ_A. By constructing a forward equation for $\mathbb{E}_x\tau_A$ based on the possible scenario's for the first step of a process starting in $x \in \mathcal{S} \setminus A$, it follows that

$$\mathbb{E}_x\tau_A = \sum_{y\in A} p(x,y) + \sum_{x\in\mathcal{S}\setminus A} p(x,y)(1 + \mathbb{E}_y\tau_A) \tag{2.33}$$

for all $x \in \mathcal{S} \setminus A$. Again, it will be convenient to define a function

$$w_A(x) := \begin{cases} \mathbb{E}_x\tau_A, & \text{if } x \in \mathcal{S} \setminus A \\ 0, & \text{if } x \in A \end{cases} \tag{2.34}$$

such that

$$w_A(x) = 1 + \sum_{y\in\mathcal{S}} p(x,y) w_A(y). \tag{2.35}$$

for $x \in \mathcal{S} \setminus A$. Therefore, the function w_A can be seen as the solution of the inhomogeneous Dirichlet problem.

$$\begin{aligned}(\mathcal{L}w_A)(x) &= 1, \quad x \in \mathcal{S} \setminus A, \\ w_A(x) &= 0, \quad x \in A.\end{aligned} \tag{2.36}$$

From Proposition 2.15 it followed that the homogeneous boundary value problem has an unique solution, implying that problem 2.36 also has an unique solution, which can be by linearity represented in the form

$$\mathbb{E}_x\tau_A = w_A(x) = \sum_{y\in\mathcal{S}\setminus A} G_{\mathcal{S}\setminus A}(x,y). \tag{2.37}$$

Where $G_{\mathcal{S}\setminus A}$ is called the *Green's function*, which is simply the matrix inverse of the *Dirichlet operator* $\mathcal{L}^{\mathcal{S}\setminus A}$ *on* $\mathcal{S} \setminus A$, a matrix whose elements are given as,

$$\mathcal{L}^{\mathcal{S}\setminus A}(x,y) = \begin{cases} \mathcal{L}(x,y) & \text{if } x,y \in \mathcal{S} \setminus A \\ 0, & \text{if } x \in A \text{ or } y \in A \end{cases} \tag{2.38}$$

Now, by starting with (2.17) and taking into account the observation that $h_{A,D}(x) = 1 - h_{D,A}(x)$, which trivially holds when stated in terms of $\mathbb{P}_x[\tau_A < \tau_D]$, it is possible to represent the Greens's function, and thus

to represent the mean value of the hitting times τ_A, in terms of equilibrium potentials, stationary distributions and capacities. To observe this, first note that,

$$e_{A,D}(x) = \mathcal{L}h_{D,A}(x). \tag{2.39}$$

With this relation, and assuming that $e_{A,D}$ is given on D, an inhomogeneous Dirichlet problem, with boundary conditions being present only on on A, can be formulated for $h_{D,A}$ as

$$\begin{aligned} (\mathcal{L}h_{D,A})(x) &= 0, && x \in \mathcal{S} \setminus (A \cup D), \\ (\mathcal{L}h_{D,A})(x) &= e_{A,D}(x), && x \in D, \\ h_{A,D}(x) &= 0, && x \in A. \end{aligned} \tag{2.40}$$

Thus,

$$h_{D,A}(x) = \sum_{y \in D} G_{\mathcal{S}\setminus A}(x,y) e_{A,D}(y). \tag{2.41}$$

Borrowing from the previous section, consider again the special case where D is a single point $y \in \mathcal{S}$, than (2.41) yields

$$G_{\mathcal{S}\setminus A}(x,y) = \frac{h_{y,A}(x)}{e_{A,D}(y)}. \tag{2.42}$$

And due to the symmetry of $\mathcal{L}$, i.e.

$$G_{\mathcal{S}\setminus A}(x,y)\mu(x) = G_{\mathcal{S}\setminus A}(y,x)\mu(y) \tag{2.43}$$

the Green's function can be given as,

$$G_{\mathcal{S}\setminus A}(y,x) = \frac{\mu(x) h_{y,A}(x)}{\mu(y) e_{A,D}(y)}. \tag{2.44}$$

Corollary 2.23. *The Dirichlet Green's function for any non-empty subset $A \subset \mathcal{S}$ can be represented in terms of the equilibrium potential, stationary distributions and capacities as*

$$G_{\mathcal{S}\setminus A}(x,y) = \frac{\mu(y) h_{x,A}(y)}{CAP(A,y)} \tag{2.45}$$

With this corollary, we now get the desired representation for the mean value of the hitting times τ_A as

$$\mathbb{E}_x \tau_A = \sum_{y \in \mathcal{S}\setminus A} \frac{\mu(y) h_{x,A}(y)}{CAP(A,y)}. \tag{2.46}$$

2.3 Metastability

Finally, we can now deal with the subject of metastability in the context of discrete Markov chains.

Definition 2.24. *Assume that $\mathcal{S}$ is a discrete set. Then a Markov process χ is called* ***metastable with respect to the set*** *$\mathcal{M} \subset \mathcal{S}$, if*

$$\frac{\sup_{x \in \mathcal{M}} \mathbb{P}_x[\tau_{\mathcal{M}\setminus x} < \tau_x]}{\inf_{y \notin \mathcal{M}} \mathbb{P}_y[\tau_{\mathcal{M}} < \tau_y]} \leq \rho \ll 1 \tag{2.47}$$

for some $\rho > 0$.

Note that the definition for metastability is given in terms of escape probabilities, therefore we can find an equivalent definition in terms of capacities, assuming that $\mathcal{S}$ is finite.

Theorem 2.25. *Assume that $\mathcal{S}$ is a finite discrete set. Then a Markov process χ is* ***metastable*** *with respect to the set $\mathcal{M} \subset \mathcal{S}$, if*

$$\frac{\max_{y \notin \mathcal{M}} \mu(y) CAP(y,\mathcal{M})^{-1}}{\min_{x \in \mathcal{M}} \mu(x) CAP(x, \mathcal{M}\setminus x)^{-1}} \leq \rho \ll 1 \tag{2.48}$$

for some $\rho > 0$.

Proof.

$$\frac{\sup_{x\in\mathcal{M}} \mathbb{P}_x[\tau_{\mathcal{M}\setminus x} < \tau_x]}{\inf_{y\notin\mathcal{M}} \mathbb{P}_y[\tau_{\mathcal{M}} < \tau_y]} = \frac{\max_{x\in\mathcal{M}} \mu(x)^{-1} CAP(x, \mathcal{M}\setminus x)}{\min_{y\notin\mathcal{M}} \mu(y)^{-1} CAP(y,\mathcal{M})} = \frac{\max_{y\notin\mathcal{M}} \mu(y) CAP(y,\mathcal{M})^{-1}}{\min_{x\in\mathcal{M}} \mu(x) CAP(x,\mathcal{M}\setminus x)^{-1}}$$

□

Henceforth, we will denote the set of metastable points by $\mathcal{M} \subset \mathcal{S}$, which allows us to define the useful notion of valleys of the metastable points.

Definition 2.26. *The **valley** (or **basin of attraction**) $A(x)$ of a point in $x \in \mathcal{M}$ is defined as*

$$A(x) := \left\{ z \in \mathcal{S} \mid \mathbb{P}_z[\tau_x = \tau_{\mathcal{M}}] = \sup_{y\in\mathcal{M}} \mathbb{P}_z[\tau_y = \tau_{\mathcal{M}}] \right\}. \tag{2.49}$$

In other words, the valley $A(x)$ of a point $x \in \mathcal{M}$ contains all $z \in \mathcal{S}$ such that

$$\mathbb{P}_z[\tau_x < \tau_{\mathcal{M}\setminus x}] \geq \mathbb{P}_z[\tau_{\mathcal{M}\setminus x} < \tau_x]. \tag{2.50}$$

Note that valleys may overlap. Although formulated in a completely probabilistic setting, it will demonstrated that valleys represent *local minima* of an energy landscape defined by some energy measure on the state space.

Lastly,

Theorem 2.27. *Let $x \in \mathcal{M}$ and $J \subset \mathcal{M}\setminus x$ be such that for all $m \in \mathcal{M}\setminus(J\cup x)$ either $\mu(m) \ll \mu(x)$ or $CAP(x,J) \gg CAP(m,x)$, then*

$$\mathbb{E}_x \tau_J = \frac{\mu(A(x))}{CAP(x,J)} (1 + o(1)). \tag{2.51}$$

Proof. See [3].

□

Henceforth, we will call the hitting times of those processes started in $x \in \mathcal{M}$ to $J \subset \mathcal{M}\setminus x$ an *exit time* of the metastable phase x. This concludes the potential theoretic approach to metastability.

3 Sharp Asymptotics for Probabilistic Cellular Automata

In this section, we introduce the basic notation, and define a specific class of reversible Probabilistic Cellular Automata, which corresponds to the parallel implementation of the Ising model in a heat bath with self-interaction.

3.1 Probabilistic Cellular Automata

First of all, let $\Lambda \subset \mathbb{Z}^2$ be a finite square of size $L \times L$ with periodic boundary conditions, i.e. the torus Λ endowed with the Euclidean measure. Associated with each *site* $x \in \Lambda$, is a *single-spin* state space given by the finite set $\mathcal{S}_0 := \{-1, +1\}$, such that the spin state variable is given by $\sigma(x) \in \mathcal{S}_0$ and denote by $\mathcal{S} := \mathcal{S}_0^\Lambda$ the state space. Furthermore, any $\sigma \in \mathcal{S}$ is called a *state* or *configuration* of the system. Moreover, given $\sigma \in \mathcal{S}$ and $x \in \Lambda$, we denote by σ^x the configuration such that $\sigma^x(x) = -\sigma(x)$ and $\sigma^x(y) = \sigma(y)$ for all $y \neq x$.

Next, introduce for any $x \in \Lambda$ the shift Θ_x on the torus, shifting a configuration in $\mathcal{S}$ such that the site x is mapped to the origin 0. More precisely

$$(\Theta_x \sigma)(y) = \sigma(x + y). \tag{3.1}$$

Let $\beta > 0$ and $h \in \mathbb{R}$ such that $|h| < 1$ and $2/h$ is not an integer, we consider the Markov chain χ with finite state space $\mathcal{S}$ and transition matrix

$$p(\sigma, \eta) \coloneqq \prod_{x \in \Lambda} p_{x,\sigma}(\eta(x)) \qquad \forall \sigma, \eta \in \mathcal{S}. \tag{3.2}$$

Here, the probability measure $p_{x,\sigma}(\cdot)$ on $\mathcal{S}_{\{x\}}$ is defined for all $x \in \Lambda$ and $\sigma \in \mathcal{S}$ as

$$p_{x,\sigma}(s) \coloneqq \frac{1}{1 + \exp\{-2\beta s\,(S_\sigma(x) + h)\}} = \frac{1}{2}[1 + s \tanh \beta(S_\sigma(x) + h)] \tag{3.3}$$

where $s \in \{-1, +1\}$ and

$$S_\sigma(x) \coloneqq \sum_{y \in \Lambda} K(y)(\Theta_x \sigma)(y) \tag{3.4}$$

the *local updating rule* with *kernel* K. The kernel K is a function such that its support is a subset of Λ and $K(x) = K(x')$ whenever $x, x' \in \Lambda$ are symmetric with respect to the origin. The choice of the kernel directly links the PCA to the corresponding implementation of the Ising model. Therefore, we consider the five site *cross* centered at the origin, i.e.

$$K(z) = \begin{cases} 1, & \text{if } z \text{ corresponds to the origin} \\ 1, & \text{if } z \text{ is a nearest neighbour of the origin} \\ 0, & \text{otherwise} \end{cases} \tag{3.5}$$

Note that the updating rule S_σ is a discrete convolution of σ given the kernel K. Furthermore, the normalisation condition $p_{x,\sigma}(s) + p_{x,\sigma}(-s) = 1$ is trivially satisfied. Indeed, the Markov chain χ described by this class of PCA is time-homogeneous, irreducible, has a discrete finite state space $\mathcal{S}$ and more importantly is reversible. Hence, all theorems concerning the potential theoretic approach, that were elaborated on in the previous section, hold.

3.1.1 The Stationary Measure

It can be proven (see [8]), provided that the kernel K is symmetric with respect to the origin, that the Markov chain χ is indeed reversible with respect to the finite volume Gibbs measure

$$\mu(\sigma) \coloneqq \frac{e^{-\beta H(\sigma)}}{Z} \tag{3.6}$$

where Z is the partition function and H the Hamiltonian defined as

$$H(\sigma) \coloneqq H_{\beta,h}(\sigma) \coloneqq -h \sum_{x \in \Lambda} \sigma(x) - \frac{1}{\beta} \sum_{x \in \Lambda} \log \cosh[\beta(S_\sigma(x) + h)]. \tag{3.7}$$

As a consequence, the detailed balance equations are satisfied, i.e.

$$p(\sigma, \eta) e^{-\beta H(\sigma)} = p(\eta, \sigma) e^{-\beta H(\eta)} \qquad \forall \sigma, \eta \in \mathcal{S}. \tag{3.8}$$

Hence, it follows from Proposition 2.9 that μ is the unique stationary distribution. Furthermore, due to the corresponding physical model, we shall refer to $1/\beta$ as to the *temperature* an to h as the *magnetic field*.

For the analysis of the problem of metastability, it is necessary to have a definition of ground states, but due to the dependence of the Hamiltonian on β, these are not trivially found. However, since the ground states are those configurations on which the Gibbs measure μ concentrates when $\beta \to \infty$, they can be defined a the minima of the *energy*

$$E(\sigma) \coloneqq \lim_{\beta \to \infty} H(\sigma) = -h \sum_{x \in \Lambda} \sigma(x) - \sum_{x \in \Lambda} |S_\sigma(x) + h|. \tag{3.9}$$

3.1.2 Communication Energies

As previously stated, allowing for simultaneous updates to the systems states breaks continuity constrains. Indeed, the energy difference between two configurations is not sufficient to describe the trajectories in the configuration space, since they may be suppressed in probability, by the law (3.2). The latter can be regarded as an additional energy barrier generated by the dynamics of the system. In fact, there are pairs of configurations such that there is a energy barrier in both directions. Hence, the dynamics cannot merely be described in terms of $H(\sigma) - H(\eta)$ alone, as usual for serial Glauber dynamics. To this end, we extend the Hamiltonian (3.7) to a sort of pairwise *communication height* $\mathcal{H}(\sigma, \eta)$ such that

$$\mathcal{H}(\sigma, \eta) \coloneqq H(\sigma) - \frac{1}{\beta} \log p(\sigma, \eta). \tag{3.10}$$

Now, we can also consider the *communication energy* as

$$\mathcal{E}(\sigma, \eta) \coloneqq \lim_{\beta \to \infty} \mathcal{H}(\sigma, \eta) \geq \max\{E(\sigma), E(\eta)\}, \tag{3.11}$$

and the *transition rate* between configurations as

$$\Delta(\sigma, \eta) \coloneqq \mathcal{E}(\sigma, \eta) - E(\sigma) = \sum_{\substack{x \in \Lambda \\ \eta(x)(S_\sigma(x)+h)<0}} 2|S_\sigma(x) + h| \geq 0. \tag{3.12}$$

A simple Lemma that relates the communication height $\mathcal{H}(\sigma, \eta)$ to the communication energy $\mathcal{E}(\sigma, \eta)$ can now be stated.

Lemma 3.1. *For any $\sigma, \eta \in \mathcal{S}$ we have*

$$\mathcal{H}(\sigma, \eta) = \mathcal{E}(\sigma, \eta) + \frac{|\Lambda| \log 2}{\beta}. \tag{3.13}$$

Proof. See Appendix A. □

Lastly, it will be useful to define trajectories in the configuration space in terms of paths.

Definition 3.2. *A finite sequence of configurations $\omega = \{\omega_1, ..., \omega_n\}$ is called a **path** with starting configuration ω_1 and ending configuration ω_n. Given a path ω we define the **height** along ω as*

$$\Phi_\omega \coloneqq \begin{cases} E(\omega_1), & \text{if } |\omega| = 1 \\ \max\limits_{i=1,\dots,n-1} \mathcal{E}(\omega_i, \omega_{i+1}), & \text{otherwise} \end{cases} \tag{3.14}$$

Furthermore, given two configurations $\sigma, \eta \in \mathcal{S}$ we donote by $\Theta(\sigma, \eta)$ the set of all paths ω starting from σ and ending in η. The minimax between σ and η is defined as

$$\Phi(\sigma, \eta) \coloneqq \min_{\omega \in \Theta(\sigma,\eta)} \Phi_\omega. \tag{3.15}$$

Finding the minimax $\Phi(\sigma, \eta)$ is arguably a particular complicated problem, since all paths between σ and η need to be considered, whereas the minimax may even be obtained on a path that is not the most direct path between the two configurations.

3.2 Main Results: Sharp Description of Nucleation

We shall now pose the problem of metastability by stating the related theorem on the exit time of the metastable phase for the model in (3.2) with $0 < h < 1$.

Suppose that the system is prepared in the state $\sigma_0 = -\underline{1}$, where $-\underline{1}$ is the phase with negative magnetisation, i.e. the configuration with all minuses, then the system tends to $+\underline{1}$, the phase with positive magnetisation

in the infinite time limit. Moreover, we shall proof that $-\underline{1}$ is metastable in the sense that the system spends a huge amount of time 'close' to $-\underline{1}$ before visiting $+\underline{1}$. More precisely, the exit time $\tau_{+\underline{1}}$ is an exponential random variable with its mean exponentially large in β.

First, let us consider the *critical length* λ defined as

$$\lambda \coloneqq \left\lfloor \frac{2}{h} \right\rfloor + 1, \tag{3.16}$$

in which $\lfloor x \rfloor$ denotes the largest integer smaller that the real x. We choose $2/h$ is not integer as to avoid ties (see [6]). Then, in order to state the main theorem for the PCA, we define the *activation energy* of the configurations that trigger nucleation as

$$\Gamma_1 \coloneqq -4h\lambda^2 + 4(4+h)\lambda + 2 - 6h, \tag{3.17}$$

corresponding to the choice of the kernel K. In particular, this corresponds to the first of model depended result outlined outlined in the introduction, for which it was proven in [6] that,

$$\lim_{\beta\to\infty} \frac{1}{\beta} \log \tau_{+\underline{1}} = \Gamma_1, \text{ and} \tag{3.18}$$

$$\lim_{\beta\to\infty} \frac{1}{\beta} \log \mathbb{E}_{-\underline{1}} \tau_{+\underline{1}} = \Gamma_1. \tag{3.19}$$

Moreover, before reaching the ground state $+\underline{1}$, the system started at $-\underline{1}$ must necessarily visit a set of critical droplets $\mathcal{C}$.

In this thesis, shaper results to that of [6] are presented, while using the almost the same model-dependent input, computing the mean transition time up to sub-exponential prefactors, and reproducing the results already obtained in [10]. Indeed, we have

Theorem 3.3 (**Main Theorem**). *Consider the probabilistic cellular automaton (3.2), and suppose $h > 0$ is chosen small enough, then*

$$\mathbb{E}_{-\underline{1}} \tau_{+\underline{1}} = K_1^{-1} e^{\beta\Gamma_1}(1 + o(1)) \tag{3.20}$$

where

$$K_1 = 2^{-|\Lambda|} 8 |\Lambda| (\lambda - 1) \tag{3.21}$$

for β large enough.

3.3 Proof of the Main Theorem

In order to prove the main theorem, we first show that the metastable set $\mathcal{M}$ is $\{-\underline{1}, +\underline{1}\}$. To do so, we first give the following definitions (see Figure 3.1).

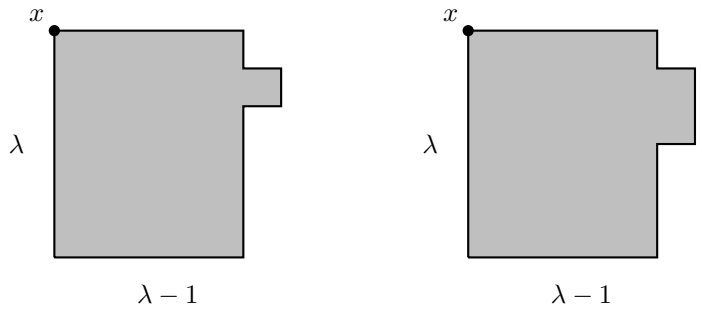

(a) A protocritical droplet $\sigma \in \mathcal{P}$ (b) A critical droplet $\eta \in \mathcal{C}$

Figure 3.1: Examples of the set of saddles

Definition 3.4 (**Saddles**).

1. *We denote by $\mathcal{P}$ the set of the* ***protocritical droplets*** *containing the configurations with all the spins equal to -1, except those in a rectangle of sides $\lambda-1$ and λ in a neighbouring site adjacent to one of the longest sites.*

2. *We denote by $\mathcal{C}$ the set of the* ***critical droplets*** *containing the configurations with all the spins equal to -1, except those in a rectangle of sides $\lambda-1$ and λ in a pair of neighbouring site adjacent to one of the longest sites.*

Now let us restate a theorem derived from [6], providing a recurrence property on the set $\{-\underline{1},+\underline{1}\}$ with respect to the set of saddles.

Theorem 3.5. *Denote by Γ_1 the activation energy defined in (3.17) and suppose $h>0$ is chosen small enough, then*

1. *for any $\sigma\in\mathcal{S}\setminus\{-\underline{1}\}$ we have*
$$\Phi(\sigma,+\underline{1})-E(\sigma)<\Gamma_1. \tag{3.22}$$

2. *we have*
$$\Phi(-\underline{1},+\underline{1})-E(-\underline{1})=\Gamma_1. \tag{3.23}$$

3. *for each path $\omega\in\Theta(-\underline{1},+\underline{1})$ such that $\Phi_\omega=\Gamma_1$, it holds that $\mathcal{E}(\omega_{i-1},\omega_i)=\Gamma_1$ if and only if $\omega_{i-1}\in\mathcal{P}$, $\omega_i\in\mathcal{C}$ and $\omega_i=\omega_{i-1}^x$ for a suitable $x\in\Lambda$.*

Proof. See [6]

□

Furthermore, the following estimate is given in [4].

Lemma 3.6. *For every non-empty disjoined subsets $A,D\subset\mathcal{S}$, there exists constants $0<C_1\le C_2<\infty$ (depending on A,D) such that for all β*
$$C_1\le e^{\beta\,\Phi(A,D)}\;Z\;CAP(A,D)\le C_2. \tag{3.24}$$

Proof. See [4].

□

Consequently, using the definition of a metastable state in (2.48).

Theorem 3.7. *Consider the probabilistic cellular automaton (3.2), suppose $h>0$ is chosen small enough, then*
$$\mathcal{M}=\{-\underline{1},+\underline{1}\}. \tag{3.25}$$
for β large enough.

Proof. From [10]. Denote by C_i any positive constant non depending on β. Then from (3.22), (3.24) and (A.2) it follows that for any $\eta\notin\{-\underline{1},+\underline{1}\}$
$$\mu(\eta)[CAP(\eta,\mathcal{M})]^{-1}\le\frac{Z}{C_1}\mu(\eta)e^{\beta\,\Phi(\eta,+\underline{1})}\le\frac{1}{C_1}e^{\beta[\Phi(\eta,+\underline{1})-H(\eta)]}\le C_3e^{\beta(\Gamma_1-\delta)} \tag{3.26}$$
for some $\delta>0$. But if $\eta\in\{-\underline{1},+\underline{1}\}$, we have
$$\mu(-\underline{1})[CAP(-\underline{1},+\underline{1})]^{-1}\ge C_4e^{\beta\Gamma_1}. \tag{3.27}$$
Indeed, if $\eta=-\underline{1}$ equation (3.27) follows from (3.22), (3.24) and (A.2), while if $\eta=+\underline{1}$, because the capacity is a symmetric function, we can write
$$\mu(+\underline{1})[CAP(-\underline{1},+\underline{1})]^{-1}\ge\frac{Z}{C_2}\frac{\mu(+\underline{1})}{e^{-\beta\,\Phi(-\underline{1},+\underline{1})}}=\frac{e^{-\beta[\Phi(+\underline{1},+\underline{1})-H(+\underline{1})]}}{C_2}>C_5e^{\beta\Gamma_1}.$$

Hence, from (3.26) and (3.27), we get

$$\frac{\max_{\eta\notin\mathcal{M}}\mu(\eta)CAP(\eta,\mathcal{M})^{-1}}{\min_{\eta\in\mathcal{M}}\mu(\eta)CAP(\eta,\mathcal{M}\setminus\eta)^{-1}}\leq C_6e^{-\beta\delta}<\rho\ll 1 \tag{3.28}$$

for β large enough, which concludes the proof. □

A simple Lemma regarding the stationary measure of the valley $A(-\underline{1})$ of the metastable state $-\underline{1}$ will proof to be necessary and is stated as

Lemma 3.8. *Consider the probabilistic cellular automaton (3.2), suppose $h>0$ is chosen small enough, then*

$$\mu(A(-\underline{1}))=\mu(-\underline{1})(1+o(1)) \tag{3.29}$$

for β large enough.

Proof. See [4].

□

3.3.1 Sharp Estimates for $CAP(-\underline{1},+\underline{1})$

Before continuing, we introduce a set $\mathcal{G}$ as in [6]. This set $\mathcal{G}\subset\mathcal{S}$, containing $-\underline{1}$, but not $+\underline{1}$, was constructed in such a way that the evaluation of the transition energy for all the possible transitions from the interior to the exterior of such a set $\mathcal{G}$ is under control. Moreover, the set $\mathcal{G}$ contains all *subcritical configurations*, i.e. those configurations $\sigma\in\mathcal{S}$ such that a process starting from σ will visit $-\underline{1}$ before $+\underline{1}$ with probability tending to one in the limit $\beta\to\infty$.

Proposition 3.9. *Consider the probabilistic cellular automaton (3.2), with $\mathcal{G}$ defined in* [6]*, suppose $h>0$ is chosen small enough and $L=L(h)$ large enough, then*

1. *$-\underline{1}\in\mathcal{G}$, $+\underline{1}\in\mathcal{S}\setminus\mathcal{G}$ and $\mathcal{C}\subset\mathcal{S}\setminus\mathcal{G}$.*
2. *for each $\sigma\in\mathcal{G}$ and $\eta\in\mathcal{S}\setminus\mathcal{G}$ we have $\mathcal{E}(\sigma,\eta)\geq E(-\underline{1})+\Gamma_1$.*
3. *for each $\sigma\in\mathcal{G}$ and $\eta\in\mathcal{S}\setminus\mathcal{G}$ we have $\mathcal{E}(\sigma,\eta)=E(-\underline{1})+\Gamma_1$ if and only if $\sigma\in\mathcal{P}$, $\eta\in\mathcal{C}$ and $\eta=\sigma^x$ for a suitable $x\in\Lambda$.*

Proof. See [6].

□

With this last proposition, all pieces of the puzzle prove the sharp estimates for the capacity between $-\underline{1}$ and $+\underline{1}$, and consequently the mean exit time.

Theorem 3.10. *With the notation of Theorem 3.3, we have*

$$CAP(-\underline{1},+\underline{1})=K_1\mu(-\underline{1})e^{-\beta\Gamma_1}(1+o(1)) \tag{3.30}$$

for β large enough.

Proof. In order to prove the theorem, we will prove upper and lower bounds to the capacity $CAP(-\underline{1},+\underline{1})$.

(i) Upper bound
From [10]. We prove an upper bound by guessing some a priori properties of the equilibrium potential h^*, i.e. the minimiser solving the variational problem (2.21). Let us therefore choose a test function h^u in the following way,

$$h^u(\sigma):=\begin{cases}1, & \text{if } \sigma\in\mathcal{G}\\ 0, & \text{if } \sigma\in\mathcal{S}\setminus\mathcal{G}\end{cases} \tag{3.31}$$

Thus, using Lemma 3.1, Proposition 3.9 and (A.2), we get

$$\begin{aligned}\mathfrak{C}(h^u) = \frac{1}{2}\sum_{\sigma,\eta\in\mathcal{S}}\mu(\sigma)p(\sigma,\eta)[h(\sigma)-h(\eta)]^2 = \frac{1}{Z}\sum_{\substack{\sigma\in\mathcal{G},\\ \eta\in\mathcal{S}\setminus\mathcal{G}}} e^{-\beta\mathcal{H}(\sigma,\eta)} &= 2^{-|\Lambda|}\frac{1}{Z}\sum_{\substack{\sigma\in\mathcal{G},\\ \eta\in\mathcal{S}\setminus\mathcal{G}}} e^{-\beta\mathcal{E}(\sigma,\eta)}\\ &\le 2^{-|\Lambda|}\mu(-\underline{1})\sum_{\substack{\sigma\in\mathcal{G},\\ \eta\in\mathcal{S}\setminus\mathcal{G}}} e^{-\beta[\mathcal{E}(\sigma,\eta)-E(-\underline{1})]}\\ &\le 2^{-|\Lambda|}\mu(-\underline{1})\left[N_1 e^{-\beta\Gamma_1} + |\mathcal{S}|e^{-\beta(\Gamma_1+\delta)}\right]\\ &\le 2^{-|\Lambda|}\mu(-\underline{1})N_1 e^{-\beta\Gamma_1}\left(1+C_1e^{-\beta\delta}\right)\end{aligned}$$

for some $\delta > 0$ and positive constant C_1. We denote by N_1, the cardinality of the set of transitions between saddles on which the minimax Γ_1 is attained precisely, i.e. the transitions such that $\eta = \sigma^x$ for a suitable $x \in \Lambda$ for configurations $\sigma \in \mathcal{P} \subset \mathcal{G}$ and $\eta \in \mathcal{C} \subset (\mathcal{S}\setminus\mathcal{G})$.

Note that the set $\mathcal{P}$ contains all rectangles $Q_{\lambda-1,\lambda}(x)$ with a single protuberance adjacent to the one of the largest sides. Since a lattice with periodic boundary conditions is considered, translational invariance on the lattice implies that at each site x two rectangular droplets $Q_{\lambda-1,\lambda}(x)$ and $Q_{\lambda,\lambda-1}(x)$ can be associated, such that x is in the lower-left corner. The number of such rectangles is

$$N_Q = 2|\Lambda|. \tag{3.32}$$

Considering that each rectangle $Q_{\lambda-1,\lambda}(x)$ or $Q_{\lambda,\lambda-1}(x)$ forms a protocritical droplet with a single protuberance at one of the largest sides, there are two ways to form a double protuberance if the original is not in a corner and one otherwise, giving the number possible transitions between a protocritical and critical droplet

$$N_S = 2(2(\lambda-2)+2). \tag{3.33}$$

Thus,

$$N_1 = N_Q N_S = 8|\Lambda|(\lambda-1) \tag{3.34}$$

Hence,

$$CAP(-\underline{1},+\underline{1}) \le K_1\mu(-\underline{1})e^{-\beta\Gamma_1}\left(1+o(1)\right) \tag{3.35}$$

for β large enough.

(ii) Lower bound

The *optimal paths*, i.e. the paths where the minimax $\Phi(-\underline{1},+\underline{1})$ is precisely attained for the nucleation of $+\underline{1}$ starting from $-\underline{1}$, are detailed in [6] (see Sect. 3.1).

Knowing these optimal paths allows us to make a judicious choice for a reduced electrical network $(\mathcal{S},\tilde{c})$ on the equivalent electrical network $(\mathcal{S},c)$ of the PCA (3.2), i.e. $\tilde{c} \le c$, which we then exploit the monotonicity of the Dirichlet form in Theorem 2.21, to proof a lower bound. We will start by connecting nodes of $\mathcal{S}$ in the sense that

$$\tilde{c}(\sigma,\eta) = \begin{cases}\mu(\sigma)p(\sigma,\eta), & \text{if } \sigma \text{ and } \eta \text{ are connected}\\ 0, & \text{otherwise}\end{cases} \tag{3.36}$$

More precisely, starting from the node $-\underline{1}$, we connect to each site x two *deterministic paths* on which either the *horizontal* quasi-square droplet with support equal to $Q_{\lambda-1,\lambda}(x)$, or the *vertical* equivalent with support equal to $Q_{\lambda,\lambda-1}(x)$ is nucleated stepwise by a single protuberance in the *canonical order*, described respectively in Figures B.1 and B.2. Next, we connect to every quasi-square droplet the associated set of protocritical droplets $\mathcal{P}$, which in turn are connected to all the possible transitions to the associated set of critical droplet $\mathcal{C}$. After which, we nucleate the super-critical square droplet with support equal to $Q_{\lambda,\lambda}(x')$, by first filling the smallest part from λ-long slice at the side of the protuberances, and after the largest part. Lastly, we connect to every super-critical droplet a *deterministic*

path which nucleates the $+\underline{1}$ configuration, also in *canonical order*, in which we grow this super-critical droplet to square $Q_{\ell+1,\ell+1}(x')$ stepwise by a single protuberance placed in the clockwise direction starting from the upper-left side and ending bottom-right side of the square, described in Figure B.3.

Now, we claim that the paths in the reduced electrical network $(\mathcal{S}, \tilde{c})$ are in the basin of attraction of $-\underline{1}$ up to the nucleation of a protocritical droplet, and from the point of the nucleation of a critical droplet in the basin of attraction of $+\underline{1}$. Although it may be evident, this claim is stronger than necessary.

Therefore, let us consider the optimal paths $\omega_1 : -\underline{1} \to \mathcal{P}$, $\omega_2 : \mathcal{P} \to \mathcal{C}$ and $\omega_3 : \mathcal{C} \to +\underline{1}$, such that by merging the paths we obtain a optimal path $\omega : -\underline{1} \to +\underline{1}$. Then, by (3.15) we can write,

$$\Phi(-\underline{1}, +\underline{1}) = \max\{\Phi(-\underline{1}, \mathcal{P}), \Phi(\mathcal{P}, \mathcal{C}), \Phi(\mathcal{C}, +\underline{1})\} = \Gamma_1 + E(-\underline{1}). \tag{3.37}$$

And since from Theorem 3.5 it follows that the minimax is only obtained on ω_2, we thus trivially conclude that

$$\Phi(-\underline{1}, \mathcal{P}) < \Gamma_1 + E(-\underline{1}), \tag{3.38}$$
$$\Phi(\mathcal{P}, +\underline{1}) = \Gamma_1 + E(-\underline{1}), \tag{3.39}$$
$$\Phi(-\underline{1}, \mathcal{C}) = \Gamma_1 + E(-\underline{1}), \text{ and} \tag{3.40}$$
$$\Phi(\mathcal{C}, +\underline{1}) < \Gamma_1 + E(-\underline{1}). \tag{3.41}$$

Let $\sigma \in \omega_1$, and for simplicity in the sequel we will denote by C_i any positive constant non depending on β. Then we can estimate the equilibrium potential h^* on this path by

$$\begin{aligned}
\mathbb{P}_\sigma[\tau_{-\underline{1}} < \tau_{+\underline{1}}] = 1 - \mathbb{P}_\sigma[\tau_{+\underline{1}} < \tau_{-\underline{1}}] \geq 1 - \frac{CAP(\sigma, +\underline{1})}{CAP(\sigma, -\underline{1})} &\geq 1 - \frac{CAP(\sigma, +\underline{1})}{CAP(-\underline{1}, \sigma)} \\
&\geq 1 - \frac{C_2}{C_3} e^{-\beta(\Phi(\sigma, +\underline{1}) - \Phi(-\underline{1}, \sigma))} \\
&\geq 1 - C_6 e^{-\beta((\Gamma_1 + E(-\underline{1})) - (\Gamma_1 + E(-\underline{1}) - \delta))} \\
&\geq 1 - C_6 e^{-\beta\delta} \\
&\geq 1 + o(1)
\end{aligned}$$

for some $\delta > 0$ and β large enough.

Similarly, let $\eta \in \omega_3$, then the equilibrium potential h^* on this path is estimated by

$$\begin{aligned}
\mathbb{P}_\eta[\tau_{-\underline{1}} < \tau_{+\underline{1}}] \leq \frac{CAP(\eta, -\underline{1})}{CAP(\eta, +\underline{1})} &\leq \frac{CAP(-\underline{1}, \eta)}{CAP(\eta, +\underline{1})} \\
&\leq \frac{C_2}{C_3} e^{-\beta(\Phi(-\underline{1}, \eta) - \Phi(\eta, +\underline{1}))} \\
&\leq C_6 e^{-\beta((\Gamma_1 + E(-\underline{1}) - (\Gamma_1 + E(-\underline{1}) - \delta))} \\
&\leq C_6 e^{-\beta\delta} \\
&\leq o(1)
\end{aligned}$$

for some $\delta > 0$ and β large enough.

Therefore we can give the following estimates of the equilibrium potential h^*,

$$\mathbb{P}_\zeta[\tau_{-\underline{1}} < \tau_{+\underline{1}}] = h^*(\zeta) = \begin{cases} 1 + o(1) & \text{if } \zeta \in \omega_1 \\ o(1) & \text{if } \zeta \in \omega_3 \end{cases} \tag{3.42}$$

for β is large enough, implying that the only relevant contributions to the capacity are by transitions from the protocritical droplets to the critical droplets.

In what follows we will misuse the definition for the set of edges Ω and extend it to include unconnected nodes.

$$\begin{aligned}\mathfrak{C}(h^*) = \frac{1}{2}\sum_{(\sigma,\eta)\in\Omega} c(\sigma,\eta)[h^*(\sigma)-h^*(\eta)]^2 &\geq \frac{1}{2}\sum_{(\sigma,\eta)\in\Omega} \tilde{c}(\sigma,\eta)[h^*(\sigma)-h^*(\eta)]^2 \\ &\geq \sum_{\sigma\in\mathcal{P},\eta\in\mathcal{C}} \tilde{c}(\sigma,\eta)[h^*(\sigma)-h^*(\eta)]^2 \\ &\geq \sum_{\sigma\in\mathcal{P},\eta\in\mathcal{C}} \mu(\sigma)p(\sigma,\eta) \\ &= 2^{-|\Lambda|}\mu(-\underline{1}) \sum_{\sigma\in\mathcal{P},\eta\in\mathcal{C}} e^{-\beta[\mathcal{E}(\sigma,\eta)-E(-\underline{1})]}\end{aligned}$$

Hence,

$$CAP(-\underline{1},+\underline{1}) \geq K_1\mu(-\underline{1})e^{-\beta\Gamma_1} \tag{3.43}$$

for β large enough.

This concludes the proof.

□

4 Simulations for Probabilistic Cellular Automata

In this section, we will analyse a class of reversible PCA by providing heuristic and numerical arguments, proving that this type of PCA exhibits a range of metastable behaviour not trivially predicted. Moreover, since they model the process of magnetic hysteresis in stochastic lattice spin systems, this class of models is very interesting on a physically level.

4.1 Algorithm and Tools

Let us consider the class of PCA in (3.2), but introduce two new local updating rules, which we will refer to as *ferromagnetic* with kernel K and *anti-ferromagnetic* with kernel $\tilde{K}$, due to the corresponding physical models, such that

$$K(z) = \begin{cases} \kappa, & \text{if } z \text{ corresponds to the origin} \\ +1, & \text{if } z \text{ is a nearest neighbour of the origin} \\ 0, & \text{otherwise} \end{cases} \tag{4.1}$$

and

$$\tilde{K}(z) = \begin{cases} \kappa, & \text{if } z \text{ corresponds to the origin} \\ -1, & \text{if } z \text{ is a nearest neighbour north or south of the origin} \\ +1, & \text{if } z \text{ is a nearest neighbour east or west of the origin} \\ 0, & \text{otherwise} \end{cases} \tag{4.2}$$

Where $\kappa \in [0,1]$ is a parameter that tunes between self-interaction and no self-interaction, and will therefore be aptly referred to as the *self-interaction parameter*. Moreover, we will restrict κ and h such that

$$S_\sigma(x) + h \neq 0 \quad \forall x \in \Lambda \text{ and } \forall \sigma \in \mathcal{S}. \tag{4.3}$$

Next, note that $\sigma \in \mathcal{S}$ can be represented as a matrix with the dimensions equal to those of the torus Λ, i.e. $[\sigma]_{i,j} = \sigma(i,j)$ with $(i,j) \in \Lambda$ with obvious notation. It will therefore be convenient to define the matrix operator S_σ instead of the local updating rule $S_\sigma(x)$, where

$$[S_\sigma]_{i,j} = S_\sigma(i,j) \tag{4.4}$$

with obvious notation.

Then, a Markov chain Monte Carlo (MCMC) method can be used to simulate the PCA dynamics (see [8]), i.e. starting from some configuration $\sigma_0 \in \mathcal{S}$ repeatedly apply the updating rule,

$$\sigma \to \operatorname{sign}\left[\left(\frac{1}{2} + \frac{1}{2}\tanh\beta[S(\sigma) + h]\right) - z\right] \tag{4.5}$$

in which z is a matrix with dimensions equal to that of σ, containing random variables uniformly distributed between 0 and 1.

We will state a simple Lemma on the dynamics, on which heuristic arguments shall be based in the sequel.

Lemma 4.1. *Consider the probabilistic cellular automaton (3.2), suppose $h > 0$ is chosen small enough and given a configuration $\sigma \in \mathcal{S}$, then there exists a unique $\eta \in \mathcal{S}$ such that $\Delta(\sigma, \eta) = 0$, i.e.*

$$\eta(x)\,(S_\sigma(x) + h) > 0 \quad \forall x \in \Lambda. \tag{4.6}$$

*Moreover, η is the unique configuration, called the **downhill image** of σ, i.e. starting from σ, the PCA can transition to η with probability tending to one in the limit $\beta \to \infty$.*

Proof. Indeed, update rule (4.5) is given by

$$\sigma(x) \to \operatorname{sign}(S_\sigma(x) + h) \tag{4.7}$$

in the limit $\beta \to \infty$.

□

Furthermore,

Definition 4.2. *The configuration $\sigma \in \mathcal{S}$ is called a **local minimum** if and only if $\Delta(\sigma, \sigma) = 0$.*

Starting from a local minimum the probability to exit such a state is exponentially small in β, since all transitions to different configurations have a strictly positive energy cost. Moreover, consider the existence $\sigma, \eta \in \mathcal{S}$ such that $\Delta(\sigma, \eta) = \Delta(\eta, \sigma) = 0$, then the chain starting in either of the two states is trapped between them due to the same reasoning, and is referred to as a *trapping pair*.

Lastly, it would be convenient to be able to analyse the timescales in which events are suppressed in probability, to see if they contribute to the metastable behaviour. Therefore, we take a look at the large β behaviour of the probability $p_{x,\sigma}$, namely

$$p_{x,\sigma}(+1) = \frac{1}{2}[1 \tanh\beta(S_\sigma(x) + h)] = \begin{cases} 1 - e^{-2\beta|S_\sigma(x)+h|}, & \text{if } S_\sigma(x) + h > 0 \\ e^{-2\beta|S_\sigma(x)+h|}, & \text{if } S_\sigma(x) + h < 0 \end{cases} \tag{4.8}$$

and trivially it holds that $p_{x,\sigma}(-1) = 1 - p_{x,\sigma}(+1)$.

4.2 Results

In this section the application for of MCMC methods will detailed in various ways, it will shown to be an apt tool for analysing finite temperature behaviour, verifying heuristic arguments with numeric results, and most importantly as a way to gain insight into the non-trivial metastable behaviour that PCA can exhibit before rigorously analysing the model.

4.2.1 The Magnetic Field h in Relation to the Main Theorem

Recall that,

Theorem 3.3 (**Main Theorem**). *Consider the probabilistic cellular automaton (3.2), and suppose $h > 0$ is chosen small enough, then*

$$\mathbb{E}_{-\underline{1}}\tau_{+\underline{1}} = K_1^{-1}e^{\beta\Gamma_1}(1 + o(1)) \tag{3.20}$$

where

$$K_1 = 2^{-|\Lambda|}8|\Lambda|(\lambda - 1) \tag{3.21}$$

for β large enough.

The following question arises from this:

Consider the probabilistic cellular automaton (3.2). When is $h > 0$ indeed chosen small enough for some β large enough such that the zero temperature behaviour is satisfied?

To answer this, let us first consider the influence of the magnetic field h, specifically state the single site local energy minima for the two metastable states $-\underline{1}$ and $+\underline{1}$ in terms of h,

$$-h\sigma(x) - |S_\sigma(x) + h| = \begin{cases} -5 + 2h, \ \forall x \in \Lambda \text{ if } \sigma = -\underline{1} \\ -5 - 2h, \ \forall x \in \Lambda \text{ if } \sigma = +\underline{1} \end{cases} \tag{4.9}$$

Hence, it is obvious that, for $h = 0$, the two metastable states would be *degenerate*, i.e. an energy level that corresponds to two or more states, and it is therefore necessary to require that $h \neq 0$ in the case of two metastable states. Additionally, taking h as negative the PCA would have $-\underline{1}$ as the ground state, thus requiring that $h > 0$.

In particular, setting $h > 0$ creates an energy gradient between the two metastable states that is directly proportional to h, one that becomes evident when the large β behaviour of $p_{x,\sigma}$ is analysed. Indeed, we see that as long as $h < 1$ and β be to at finite temperature, the probability of a spin flip is given by a majority rule on the neighbourhood, hence the influence due to the thermal fluctuations in relation to the majority rule at the zero temperature limit can be estimated as a multiplicative error proportional to $e^{+\beta h}$. Consequently, h should be chosen small enough, implying an inverse relation between β and h.

Support this claim with a numerical result, we design a MCMC simulation in *Mathematica* for studying the exit times $\tau_{+\underline{1}}$ of the negative magnetised metastable phase $-\underline{1}$, in relation to the magnetic field $h > 0$ at different temperatures β. The difficulty of this design is finding a sharp condition for recognising the positive magnetised metastable phase $+\underline{1}$. To overcome this obstacle, we make use of *Mathematica*'s image processing features to find the size of the maximum connected cluster of minuses, and condition this to be bigger than some threshold if and only if the positive magnetised metastable phase is reached, stopping the simulation when false. The MCMC outputs the number of iterations performed. By repeating the MCMC simulation n times for a specific tuple (β, h), an estimation for the value of $\mathbb{E}_{-\underline{1}}(\tau_{+\underline{1}})$ at this tuple is obtained by taking the mean of the outputs.

Since the metastable phase behaviour corresponds to implementation of the Ising model, one expect that there exists some critical temperature T_c, such that for $T < T_c$ the system is in the *ferromagnetic* phase, i.e. it can exhibit spontaneous alignment of the spins such that the total magnetisation is non-zero in the presence of an external magnetic field. To ensure the ferromagnetic phase behaviour it is empirically established for which $T < T_c$.

The numerical results of this experiment are show Figure 4.1.

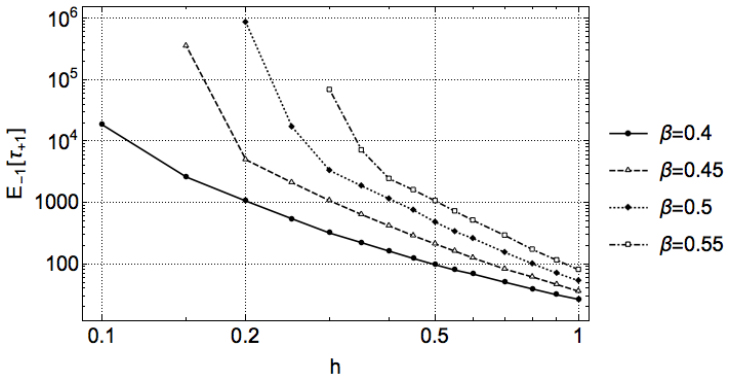

Figure 4.1: *Log-Log plot depicting the dependence of the estimated (mean) hitting time* $\hat{\mathbb{E}}_{-\underline{1}}(\tau_{+\underline{1}})$ *on the magnetic field* $h > 0$*, at different temperatures* β *with* $n = 10$*.*

Although only heuristic arguments can be made upon the results shown above, one way of interpreting the dependence of h might be, that it goes at least in terms of h as,

$$\mathbb{E}_{-\underline{1}}(\tau_{+\underline{1}}) \propto e^{+\beta/h}. \tag{4.10}$$

This would support the claim of a inverse relation between β and h. Moreover, it would also allow for the estimation of when h is small enough, i.e. choose the quotient β/h such that $e^{+\beta/h}$ is comparable in size to that of the expression found in (3.20).

4.2.2 Non Trivial Metastable Behaviour of the Ferromagnetic Case with $\kappa \in (0, 1)$

Aside from a rigorours analysis of metastable behaviour, heuristic arguments for characterising local minima can proof that intermediate states are visited during the transition from a metastable to a stable state. To demonstrate how this might be done we shall reproduce the results found in [5]. Herein the metastable behaviour is proved to be dependent on the ratio between the magnetic field and the self-interaction.

It will be convenient to introduce shorthand notations for those configurations that are local minima of the energy. Note that for $h > 0$ the configuration $\mathbf{u}$, with $\mathbf{u}(x) = +1$ for all $x \in \Lambda$, is the unique ground state, indeed each site contributes exactly $-(4 + \kappa + 2h)$. Hence, for $h = 0$ and $\kappa \in (0, 1]$, the ground states are given by $\mathbf{u}$ and $\mathbf{d}$ whereas $\mathbf{d} = +1$ for all $x \in \Lambda$. Moreover, in the case that $\kappa = 0$, the configurations $\mathbf{c}^e$ and $\mathbf{c}^o$ such that $\mathbf{c}^e(x) = (-1)^{x_1+x_2}$, respectively $\mathbf{c}^o(x) = (-1)^{x_1+x_2+1}$ for all $x = (x_1, x_2) \in \Lambda$, are also ground states. Note that $\mathbf{c}^e$ and $\mathbf{c}^o$ resemble *chessboard*-like states, i.e. $\mathbf{c}^e$ is the configuration with pluses on the even lattice positions of Λ and minuses on its complement, thus we say that $\mathbf{c}^e$ and $\mathbf{c}^o$ are of different parity, or each others spin-flipped and set $\mathbf{c} = \{\mathbf{c}^e, \mathbf{c}^o\}$.

We shall distinguish between two cases to illustrate this.

(i) *Case* $h > \kappa \geq 0$*.*

Recall the definition of a local minima, and note that the sign of $S_\sigma(x) + h$ equals to the majority of the spins in the neighbourhood associated to x by the ferromagnetic kernel. Hence, it is negative if and only if at least three spins within the neighbourhood are negative, and positive if and only if at least two are positive. This implies that the local minima are given by $\mathbf{u}$ and $\mathbf{d}$.

Furthermore,

$$E(\mathbf{d}) = (-4 - \kappa + 2h)|\Lambda|, \tag{4.11}$$
$$E(\mathbf{c}) = (-4 + \kappa)|\Lambda|, \tag{4.12}$$
$$E(\mathbf{u}) = (-4 - \kappa - 2h)|\Lambda|. \tag{4.13}$$

such that in this case, $E(\mathbf{d}) > E(\mathbf{c}) > E(\mathbf{u})$, and thus an optimal path could be constructed from $\mathbf{d}$ to $\mathbf{u}$ while visiting $\mathbf{c}$.

A path from $\mathbf{d}$ to $\mathbf{c}$ can be constructed by inserting a sequence of rectangles $Q_{\ell,m}$ of the chessboard phase into a minus background (*chessboard-minus* droplets). Although such configurations are not local minima, they do behave like trapped pairs, where the chessboard droplet within a sea of minuses continuously flips parity. This behaviour remains as the droplet grows to $\mathbf{c}$. Then, by using (3.9), the difference of energy between two chessboard-minus droplets, respectively given by $Q_{\ell,m}(\mathbf{c})$ and $Q_{\ell,m+1}(\mathbf{c})$ with $\ell, m \geq 2$, is equal to $-2(h-\kappa)\ell + 4$. Here, the first term is due to adding a ℓ-long slice, and the second term is due to the parity switch of the corners to the right side. Thus, the energy of a chessboard-minus droplet is decreased by adding an ℓ-long slice if and only if this energy difference is positive, and thus we set

$$\ell \geq \lfloor 2/(h-\kappa) \rfloor + 1 = \lambda_{\mathbf{d}}^{\mathbf{c}}. \tag{4.14}$$

Where $\lambda_{\mathbf{d}}^{\mathbf{c}}$ is the critical length for the chessboard-minus droplet, such that the activation energy between $\mathbf{d}$ and the smallest supercritical chessboard-minus droplet is equal to

$$\Gamma_{\mathbf{d}}^{\mathbf{c}} = 8/(h-\kappa). \tag{4.15}$$

Similar, a path from $\mathbf{c}$ to $\mathbf{d}$ can be constructed by inserting a sequence of rectangles $Q_{\ell,m}$ of the pluses into a chessboard background (*plus-chessboard* droplets). These configurations again behave like trapped pairs flipping parity. Then, the difference of energy between two plus-chessboard droplets respectively given by $Q_{\ell,m}(\mathbf{u})$ and $Q_{\ell,m+1}(\mathbf{u})$ with $\ell, m \geq 2$ is equal to $-2(h+\kappa)\ell + 4$. Therefore we set

$$\ell \geq \lfloor 2/(h+\kappa) \rfloor + 1 = \lambda_{\mathbf{c}}^{\mathbf{u}}, \text{ and } \Gamma_{\mathbf{c}}^{\mathbf{u}} = 8/(h+\kappa). \tag{4.16}$$

Alternatively, a direct path from $\mathbf{d}$ to $\mathbf{u}$ can be constructed by inserting a sequence of rectangles $Q_{\ell,m}$ of the pluses into a minus background (*plus-minus* droplets). Again, we can proof that the difference of energy between two plus-chessboard droplets respectively given by $Q_{\ell,m}(\mathbf{u})$ and $Q_{\ell,m+1}(\mathbf{u})$ with $\ell, m \geq 2$ is equal to $4(2 - h\ell)$. And thus we recover the result found in (3.16), namely

$$\ell \geq \lfloor 2/h \rfloor + 1 = \lambda_{\mathbf{d}}^{\mathbf{u}}, \text{ and } \Gamma_{\mathbf{d}}^{\mathbf{u}} = 16/h. \tag{4.17}$$

And lastly, a a direct path from $\mathbf{d}$ to $\mathbf{u}$ can be constructed by inserting a sequence of rectangular *frames* $Q_{\ell,m}$ with a boarder of depth one of the chessboard phase, and a internal rectangle $Q_{\ell-1,m-1}$ of pluses into the background of minuses (*frame-minus* droplet). These are peculiar configurations that also behave like trapped pairs, flipping the parity of the boarder. Analogously, we proof that the difference of energy between two frame-minus droplets respectively given by $Q_{\ell,m}(\mathbf{u})$ and $Q_{\ell,m+1}(\mathbf{u})$ with $\ell, m \geq 2$ is equal to $8 - 4(h-\kappa) - 4h\ell$. Therefore, we set

$$\ell \geq \lfloor (2 - h + \kappa)/h \rfloor + 1 = \lambda_{\mathbf{d}}^{\mathbf{f}}, \text{ and } \Gamma_{\mathbf{d}}^{\mathbf{f}} = 16[1 - (h-\kappa)/2]^2/h. \tag{4.18}$$

Before summarising these results, note that the paths from $\mathbf{d}$ to $\mathbf{u}$ that have the smallest energy difference between the supercritical droplet and $\mathbf{u}$ will be the optimal paths. Therefore, let $a = h/\kappa$ for h chosen small enough as a function of a, then the metastable behaviour depends on the ratio between the magnetic field and the self-interaction, as claimed in the beginning of this section. Analysing the energy differences we conclude there are two regimes of the parameter a where we find different types of optimal paths, in particular, consider $1 < a < 2$ and $a > 2$.

(a) For $1 < a < 2$, it holds that $\Gamma_{\mathbf{d}}^{\mathbf{f}} < \Gamma_{\mathbf{d}}^{\mathbf{u}} < \Gamma_{\mathbf{d}}^{\mathbf{c}}$. This implies that a chain starting in $\mathbf{d}$ will escape to $\mathbf{u}$ by forming a sequence of increasing frame-minus droplets, thereby nucleating the $\mathbf{u}$ phase.

(b) For $a > 2$, it holds that $\Gamma_{\mathbf{d}}^{\mathbf{c}} < \Gamma_{\mathbf{d}}^{\mathbf{f}} < \Gamma_{\mathbf{d}}^{\mathbf{u}}$. And thus a chain starting in $\mathbf{d}$ will escape to $\mathbf{u}$ by forming a sequence of increasing chessboard-minus droplets, hereafter it will form a sequence of increasing plus-chessboard droplets nucleating the $\mathbf{u}$ phase.

(c) Moreover, $\Gamma^{\mathbf{f}}_{\mathbf{d}} < \Gamma^{\mathbf{u}}_{\mathbf{d}}$ for h, κ small. So, in non of the cases will a plus-minus droplet nucleate to g the $\mathbf{u}$ phase.

These conclusions can be verified at finite temperature via a MCMC simulation. Let us first consider the detection of a chessboard frame around a plus droplet for $1 < a < 2$, note that for such a frame to exist a specific pattern should present its self at the boarders of the droplet, see Figure 4.2.

$$\begin{array}{ccc} - & + & + \\ - & - & + \\ - & + & + \end{array}$$

Figure 4.2: A boarder permutation of a frame-droplet

By finding a kernel that promotes these patterns when convolving the matrix σ (see ω in Appendix D), which we will refer to a *mask*, the existence of a boarder can be deduced. Although this cannot be quantitatively measured, a comparison between the nucleation processes depicted in Figure 4.3 makes a strong agreement that indeed a frame is formed for $1 < a < 2$.

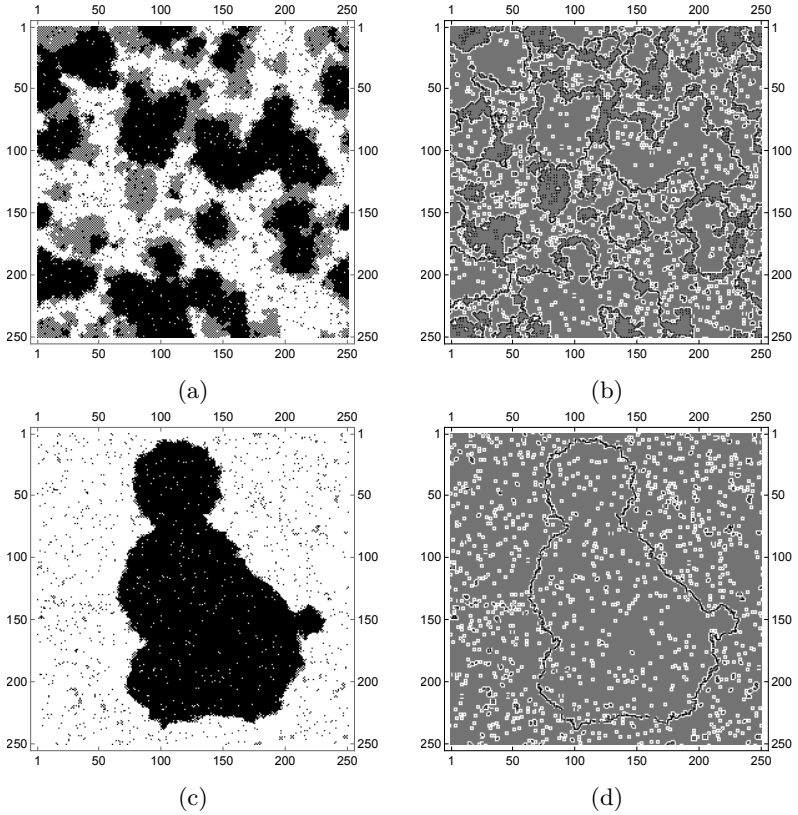

Figure 4.3: Typical results of MCMC simulations at $(\beta, h) = (0.55, 0.2)$ stopped at some time before reaching the positive magnetised phase, displaying configuration σ and the mask promoting the frame patterns, for $a > 0$ with $\kappa = 0.15$, respectively displayed by (a) and (b), and $1 < a < 2$ with $\kappa = 0.05$, respectively displayed by (c) and (d). White and black points represent respectively minus and plus spins for the configurations, and for the masks the shade of grey is proportional to the value promoting the frames.

A similar strategy can be employed to find the total magnetisation of the chessboard phase (see $\mathbf{m}\phi[\mathbf{A}, \mathbf{c}]$ in D). Then, by collecting the total magnetisation of the positive phase, and the chessboard phase together with number of iterations performed, every few iterations during the MCMC simulation, the metastable phase transitions can be plotted over time. The results can be found in Figure 4.4.

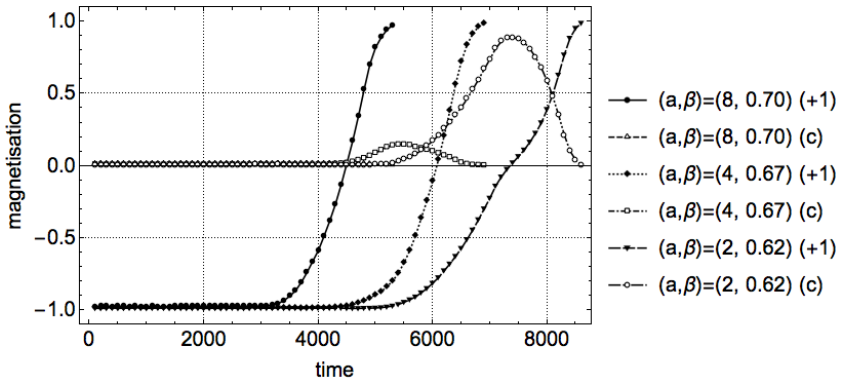

Figure 4.4: A plot of the metastable phase transition through time with $h = 0.2$. Here the total magnetisation of configuration is displayed by those curves that are labeled $+1$ and the percentage of magnetised chessboard phase by those curves that are labeled c.

It is clear that for values of $a > 2$, the intermediate chessboard $\mathbf{u}$ is indeed visited, thus confirming the heuristic arguments.

(ii) *Case* $h < \kappa \leq 1$.
Note that in this case $E(\mathbf{c}) > E(\mathbf{d}) > E(\mathbf{u})$, moreover, we restate our observations on the activation energies, thus

(a) it holds that, $\Gamma^{\mathbf{c}}_{\mathbf{d}} < 0$. This implies together with the fact that $\mathbf{c}$ has a higher energy than $\mathbf{c}$ the system cannot be trapped in chessboard-minus droplets.

(b) it holds that, $\Gamma^{\mathbf{u}}_{\mathbf{d}} < \Gamma^{\mathbf{f}}_{\mathbf{d}}$. Implying that a chain starting in $\mathbf{d}$ will escape to $\mathbf{u}$ by by forming a sequence of increasing plus-minus droplets, thereby nucleating the $\mathbf{u}$ phase.

Indeed, for $\kappa = 1$ these results are recovered. Although, the activation energy is given differently in this case, since the set of saddles is not correct in this heuristic approach, this type of reasoning provides a first approximation to the metastable behaviour.

Having considered these two distinct cases, it is evident that the PCA show a variety of different metastable scenario's.

4.2.3 Parity Interactions for the Ferromagnetic Case with $1 < a < 2$

Another example of the applications of finite temperature MCMC simulations can be found by monitoring the ferromagnetic case for $1 < a < 2$ where the intermediate chessboard phase contributes to the nucleation of the positive magnetised phase. In these cases, it can sporadically be observed that 'colliding' chessboard droplet form the plus phase at the interaction boundary, which is a dynamic interaction that is not trivially predicted. An example of this interaction is shown in Figure 4.5.

At closer inspection, one suspects that this interaction on the boarder is the result of two chessboard droplets of different parity. To investigate this, we design the following experiment with the MCMC simulation, consider the configuration with all spins -1 and place two chessboard droplets of different parity in the background. Our suspicion is confirmed after monitoring this experiment (see Figure C.1). Knowing the parity difference is responsible, we can use the downhill image (or the local updating rule at $\beta \to \infty$) to investigate what drives this behaviour and whether it is a high-temperature artefact. It will be convenient to assume $\kappa = 0$ and $0 < h < 1$.

Let us consider the interaction boarder between two chessboard droplets of different parity, the downhill image is than given by the majority rule, hence both chessboard droplet are trapped and will flip parity with

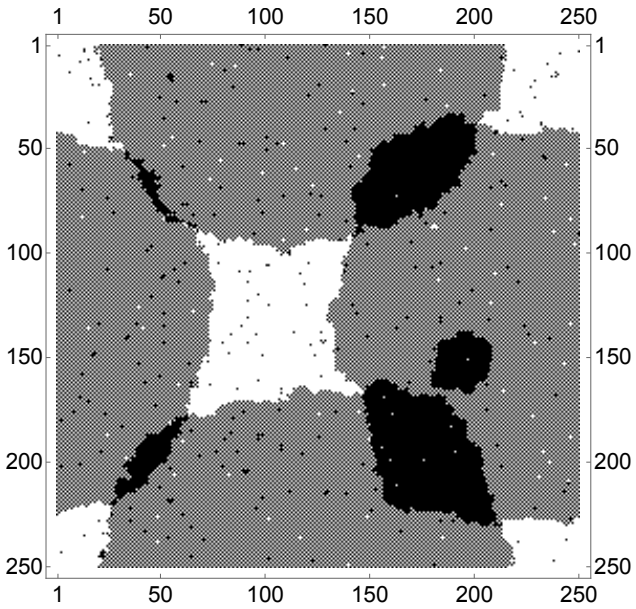

Figure 4.5: An example of the interaction of 'colliding' chessboard droplets. White and black points represent respectively minus and plus spins.

every update. Now assume a plus at the boarder does not flip parity, as shown in the first step in Figure 4.6 by the circled plus, the probability for this event happening for β large enough is proportional to

$$e^{-2\beta(2-h)} \tag{4.19}$$

But given that this event happened, the downhill images will nucleate a stripe of plusses along the interaction boundary, as shown in the consequent steps Figure 4.6 by the circled plusses.

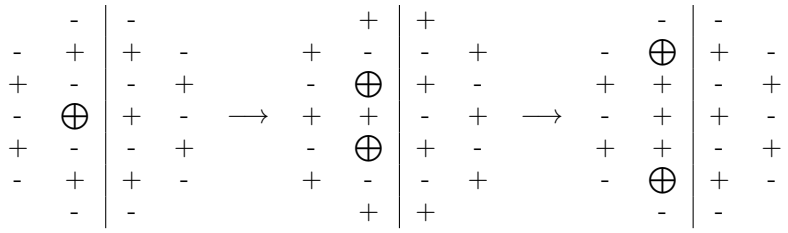

Figure 4.6: The downhill images of the interaction between two chessboard droplets of different parity, given the event that one plus on the interaction boarder remains plus.

More interestingly, the stripe is exactly nucleated along the interaction boundary, such that we can consider the 'overlap' between two nucleated chessboard droplets, i.e. the overlap of growth the two droplets if the other was not there, which can be clearly seen in Figure C.1. Testing this behaviour with the use of downhill images, it becomes apparent that the configurations at the edges of the boundaries are stable, such that the plus droplets indeed grow an overlap.

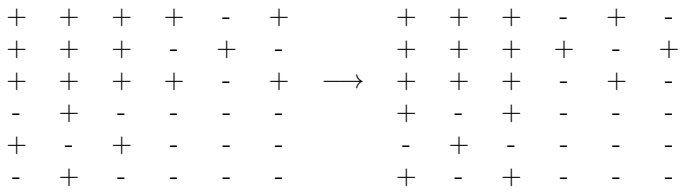

Figure 4.7: The downhill images of the interaction along the interaction boundary between two chessboard droplets, a plus droplet and a minus droplet.

The following question, given the heuristic treatment of this model in the previous section, arises from this:

Does the interaction between two chessboard-minus droplets allow for path with a lower activation energy for the nucleation of the plus one phase than previously mentioned?

The treatment of this question however is beyond the scope of this thesis.

4.2.4 Metastable States for the Anti-Ferromagnetic Case

In this section, we will treat the case of anti-ferromagnetisation, i.e. the spontaneous alignment of the spins such that the total magnetisation is zero in the presence of an external magnetic field. More precisely, we consider the PCA in (3.2) with the anti-ferromagnetic kernel $\tilde{K}$ and $\kappa > 0$ to ensure that the ground state is non-degenerate. The question we will try to address:

What are the metastable states of this model, and do there exist intermediate states the model visits during the transition of a metastable state to the stable state?

To answer this, we shall use numerical results for which we then find heuristic arguments. But first let us introduce additional shorthand notations for configurations of interest, i.e. let $\mathbf{v}^e$ and $\mathbf{v}^o$ such that $\mathbf{v}^e = (-1)^{x_1}$, respectively $\mathbf{v}^o = (-1)^{x_1+1}$ for all $(x_1, x_2) \in \Lambda$. Note that $\mathbf{v}^e$ and $\mathbf{v}^o$ resemble a state with *vertical stripes*, i.e. $\mathbf{v}^e$ is the configuration with plusses on the even vertical lattice positions of Λ and minuses on its complement, hence $\mathbf{v}^e$ and $\mathbf{v}^o$ are each others spin-flipped and we set $\mathbf{v} = \{\mathbf{v}^e, \mathbf{v}^o\}$. A similar definition can be given for the *horizontal stripes* configurations $\mathbf{h}^e$ and $\mathbf{h}^o$, such that $\mathbf{h}^e = (-1)^{x_2}$, respectively $\mathbf{h}^o = (-1)^{x_2+1}$ for all $(x_1, x_2) \in \Lambda$, and set $\mathbf{h} = \{\mathbf{h}^e, \mathbf{h}^o\}$.

The energy of these configurations in relation to the anti-ferromagnetic kernel are given as,

$$E(\mathbf{d}) = \begin{cases} \kappa|\Lambda|, & \text{if } h > \kappa \geq 0 \\ (-\kappa + 2h)|\Lambda|, & \text{if } h < \kappa \leq 1 \end{cases} \tag{4.20}$$

$$E(\mathbf{c}) = \begin{cases} -h|\Lambda|, & \text{if } h > \kappa \geq 0 \\ -\kappa|\Lambda|, & \text{if } h < \kappa \leq 1 \end{cases} \tag{4.21}$$

$$E(\mathbf{u}) = (-\kappa - 2h)|\Lambda| \tag{4.22}$$

$$E(\mathbf{v}) = (-4 + \kappa)|\Lambda| \tag{4.23}$$

$$E(\mathbf{h}) = (-4 - \kappa)|\Lambda| \tag{4.24}$$

The following step is identifying the local minima, i.e. those configurations that are there own downhill image, of the energy landscape. It immediately follows that $\mathbf{u}$ is the downhill image of $\mathbf{d}$ and therefore excludes $\mathbf{d}$ from the set of metastable phase. Thus, only considering the potential local minima, we get that $E(\mathbf{c}) > E(\mathbf{u}) > E(\mathbf{v}) > E(\mathbf{h})$, implying that possibly a optimal path could be constructed from $\mathbf{c}$ to $\mathbf{h}$ which first visits $\mathbf{u}$ and $\mathbf{v}$.

This hypothesis can be examined by designing the following MCMC simulation, starting from any of the potential local minima other than $\mathbf{h}$, does the system exhibit metastable behaviour, i.e. does the system

persist in a state that is not the ground state for a huge amount of time. This can be quantitatively analysed by considering the percentages of magnetisation of the total system by the phases in question. The results are shown in Figures 4.9, 4.8 and 4.10.

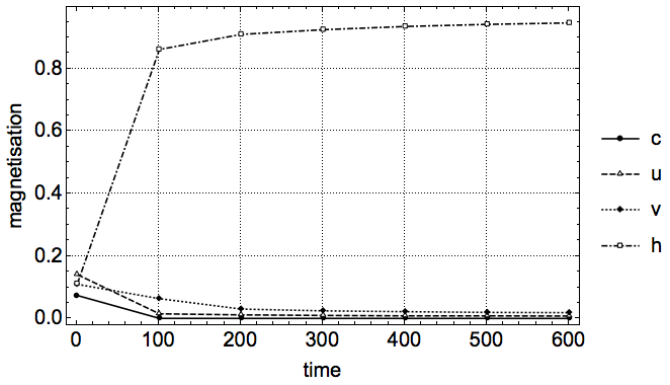

Figure 4.8: A plot of the metastable phase transition through time for a process started at **c** with $\beta = 0.7$, $h = 0.2$ and $\kappa = 0.16$. Here the total magnetisation of configuration is displayed by the curve labeled **u**, and respectively the percentage of magnetised chessboard phase, the horizontal striped phase and vertical striped phase by those curves labeled **c**, **v** and **h**.

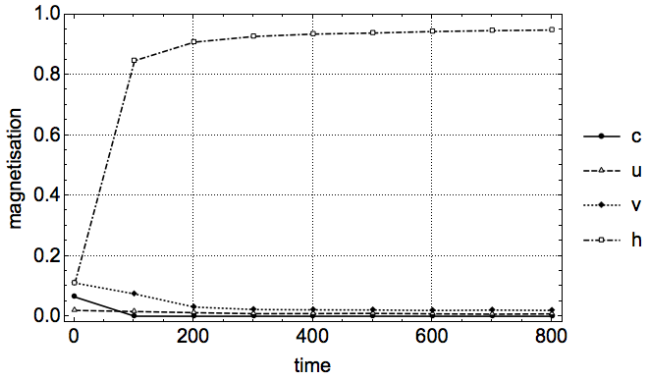

Figure 4.9: A plot of the metastable phase transition through time for a process started at **u** with $\beta = 0.7$, $h = 0.2$ and $\kappa = 0.16$. Here the total magnetisation of configuration is displayed by the curve labeled **u**, and respectively the percentage of magnetised chessboard phase, the horizontal striped phase and vertical striped phase by those curves labeled **c**, **v** and **h**.

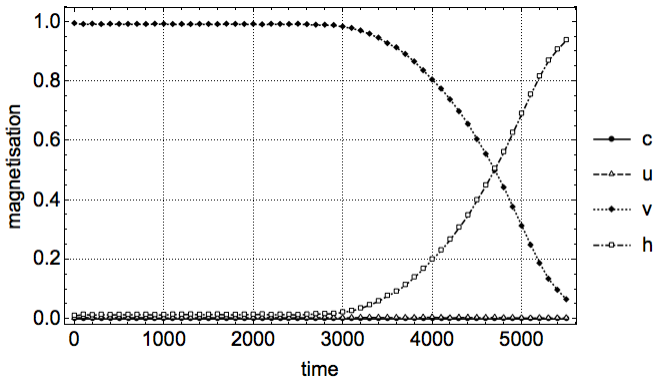

Figure 4.10: A plot of the metastable phase transition through time for a process started at $\mathbf{v}$ with $\beta = 0.7$, $h = 0.2$ and $\kappa = 0.16$. Here the total magnetisation of configuration is displayed by the curve labeled $\mathbf{u}$, and respectively the percentage of magnetised chessboard phase, the horizontal striped phase and vertical striped phase by those curves labeled $\mathbf{c}$, $\mathbf{v}$ and $\mathbf{h}$.

Analysing the figures it appears clear that neither $\mathbf{c}$ nor $\mathbf{u}$ is a metastable state for the case that $h > \kappa > 0$. Since in the $h < \kappa \leq 1$ case, the downhill images and the order of the energies associated with the phases does not change, we claim that also neither $\mathbf{c}$ nor $\mathbf{u}$ is a metastable state for $h < \kappa \leq 1$.

Given this insight into the dynamics of the system, note that in both cases the set $\mathbf{v}$ is a trapped pair, which continues to flip-flip its spins even if sequence of a rectangles $Q_{\ell,m}$ of horizontal stripes is put into the background (*horizontal-vertical striped* droplets), forming a path from $\mathbf{v}$ to $\mathbf{h}$. Then, by using (3.9), the difference of energy between two horizontal-vertical striped droplets respectively given by $Q_{\ell,m}(\mathbf{h})$ and $Q_{\ell,m+1}(\mathbf{h})$ with $\ell, m \geq 2$ is equal to $+4 - 2h - 2\kappa\ell$. Thus the energy of a horizontal-vertical striped droplet is decreased by adding an ℓ-long slice if and only if this energy difference is positive, and thus we set,

$$\ell \geq \lfloor (2-h)/\kappa \rfloor = \lambda_{\mathbf{v}}^{\mathbf{h}}. \tag{4.25}$$

Where $\lambda_{\mathbf{v}}^{\mathbf{h}}$ is the critical length for the horizontal-vertical striped droplet such that the activation energy between $\mathbf{v}$ and the smallest supercritical horizontal-vertical striped droplet is equal to

$$\Gamma_{\mathbf{v}}^{\mathbf{h}} = 2(2-h)^2/\kappa. \tag{4.26}$$

Hence, the tunnelling time is $e^{\beta \Gamma_{\mathbf{v}}^{\mathbf{h}}}$ in the sense of (3.18). Interestingly enough the tunnelling time is inversely related to the self-interaction parameter κ instead of the magnetic field h in the ferromagnetic case. The last question that now should be answered is:

Does a rigorous analysis of the zero temperature limit reveal the same conclusion on the metastable behaviour?

Again, the treatment of this question however is beyond the scope of this thesis.

A Proof of Lemma 3.1 (See page 11)

Lemma 3.1. *For any $\sigma, \eta \in \mathcal{S}$ we have*

$$\mathcal{H}(\sigma,\eta) = \mathcal{E}(\sigma,\eta) + \frac{|\Lambda|\log 2}{\beta}. \tag{3.13}$$

Proof. From [10]. By using (3.10), (3.2), (3.3) and (3.12) it follows that

$$\begin{aligned}
&\mathcal{H}(\sigma,\eta) - H(\sigma) - [\mathcal{E}(\sigma,\eta) - E(\sigma)] \\
&\qquad = -\frac{1}{\beta}\log p(\sigma,\eta) - \Delta(\sigma,\eta) \\
&\qquad = \frac{1}{\beta}\sum_{x\in\Lambda}\log(1+e^{-2\beta\eta(x)[S_\sigma(x)+h]}) + \sum_{\substack{x\in\Lambda \\ \eta(x)(S_\sigma(x)+h)<0}} 2\eta(x)[S_\sigma(x)+h] \\
&\qquad = \frac{1}{\beta}\sum_{\substack{x\in\Lambda \\ \eta(x)(S_\sigma(x)+h)>0}} \log(1+e^{-2\beta\eta(x)[S_\sigma(x)+h]}) + \frac{1}{\beta}\sum_{\substack{x\in\Lambda \\ \eta(x)(S_\sigma(x)+h)<0}} \log(1+e^{-2\beta\eta(x)[S_\sigma(x)+h]}) \\
&\qquad\quad + \sum_{\substack{x\in\Lambda \\ \eta(x)(S_\sigma(x)+h)<0}} 2\eta(x)[S_\sigma(x)+h] \\
&\qquad = \frac{1}{\beta}\sum_{\substack{x\in\Lambda \\ \eta(x)(S_\sigma(x)+h)>0}} \log(1+e^{-2\beta\eta(x)[S_\sigma(x)+h]}) + \frac{1}{\beta}\sum_{\substack{x\in\Lambda \\ \eta(x)(S_\sigma(x)+h)<0}} \log(e^{+2\beta\eta(x)[S_\sigma(x)+h]}+1) \\
&\qquad = \frac{1}{\beta}\sum_{x\in\Lambda}\log(1+e^{-2\beta|S_\sigma(x)+h|})
\end{aligned} \tag{A.1}$$

Moreover, since

$$\begin{aligned}
H(\sigma) :&= -\frac{1}{\beta}\sum_{x\in\Lambda}\log\cosh(\beta(S_\sigma(x)+h)) - h\sum_{x\in\Lambda}\sigma(x) \\
&= -\frac{1}{\beta}\sum_{x\in\Lambda}\log\cosh(\beta|S_\sigma(x)+h|) - h\sum_{x\in\Lambda}\sigma(x)
\end{aligned}$$

the difference between the Hamiltonian and the energy yields

$$\begin{aligned}
H(\sigma) - E(\sigma) &= -\frac{1}{\beta}\left[\sum_{x\in\Lambda}\log\cosh(\beta|S_\sigma(x)+h|) - \beta\sum_{x\in\Lambda}|S_\sigma(x)+h|\right] \\
&= -\frac{1}{\beta}\left[\sum_{x\in\Lambda}\Big(\log\cosh(\beta|S_\sigma(x)+h|) - \log e^{\beta|S_\sigma(x)+h|}\Big)\right] \\
&= -\frac{1}{\beta}\left[\sum_{x\in\Lambda}\left(\log\frac{1+e^{-2\beta|S_\sigma(x)+h|}}{2}\right)\right] > 0
\end{aligned} \tag{A.2}$$

By summing (A.1) and (A.2) we get

$$\mathcal{H}(\sigma,\eta) - \mathcal{E}(\sigma,\eta) = \frac{|\Lambda|\log 2}{\beta}, \tag{A.3}$$

which concludes the proof. □

B Deterministic Paths for the Reduced Network $(\mathcal{S}, \tilde{c})$

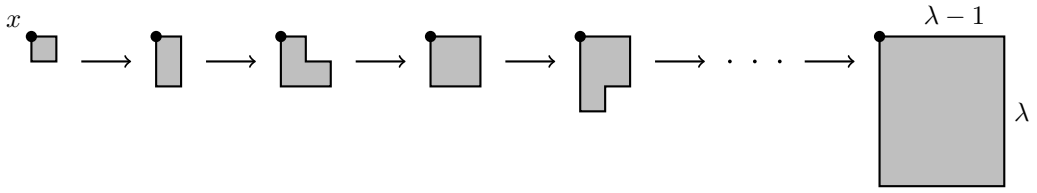

Figure B.1: The deterministic path, starting at x, for nucleating the horizontal quasi-square droplet with support equal to $Q_{\lambda-1,\lambda}(x)$

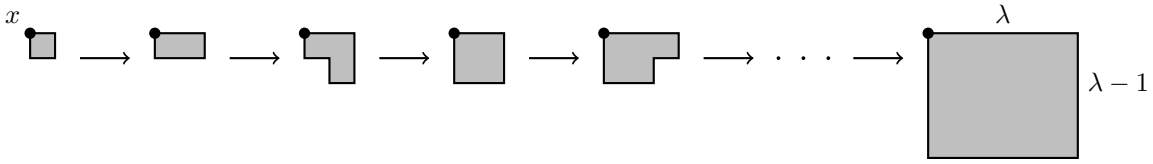

Figure B.2: The deterministic path, starting at x, for nucleating the vertical quasi-square droplet with support equal to $Q_{\lambda,\lambda-1}(x)$

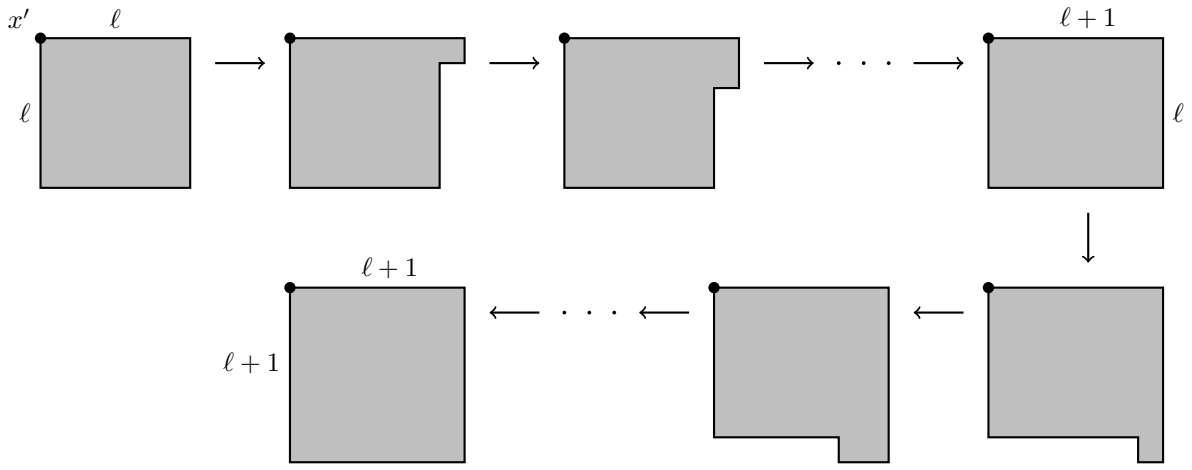

Figure B.3: The deterministic path for growing the super-critical droplet to support equal to $Q_{\ell+1,\ell+1}(x)$

C Parity Interaction of Chessboard Droplets

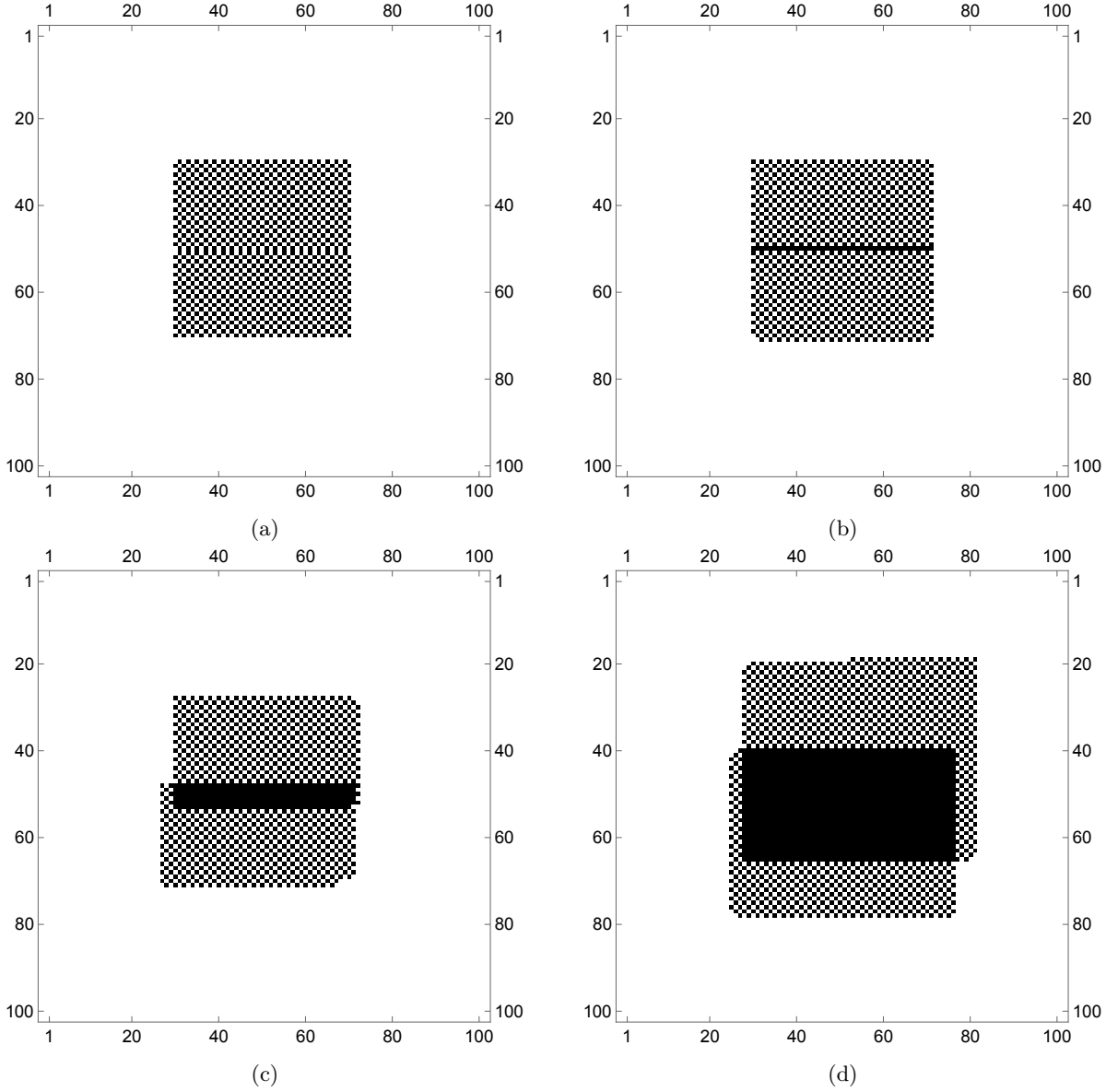

Figure C.1: The results of an experiment investigating the interaction of two chessboard droplets of different parity for $(\beta, h, \kappa) = (3, 0.2, 0)$. Here the figures (a), (b), (c) and (d) are in chronological order. White and black points represent respectively minus and plus spins.

D Mathematica Code for MCMC Simulations

Application Support

```
convolve[A_, k_] := ListCorrelate[k, A, {2, 2}]
Cardinality[A_] := Length[Flatten[A]]
```

```
S[A_] := κ A + convolve[A, k];
p[A_] := 1 / 2 (1 + Tanh[β (S[A] + h)])
```

```
c = Array[Mod[Plus[##], 2] &, {3, 3}];
a = Array[Mod[#1, 2] &, {3, 3}];
b = Array[Mod[#2, 2] &, {3, 3}];
```

```
 θ[A_] :=
  With[{B = +A + convolve[A, c]}, MorphologicalComponents[Binarize[Image[B], 4]]]
mθ[A_] := With[{B = +A + convolve[A, c]},
   Total[Binarize[Image[B], 4]] / Length[Flatten[A]]]
iθ[A_] := With[{B = +A + convolve[A, c]} ,
   MorphologicalComponents[ColorNegate[Binarize[Image[B], 4]]]]

 ϕ[A_, k_] :=
  With[{B = -A convolve[A, k]}, MorphologicalComponents[Binarize[Image[B], 3]]]
mϕ[A_, k_] := With[{B = -A convolve[A, k]},
   Total[Binarize[Image[B], 3]] / Length[Flatten[A]]]
iϕ[A_, k_] := With[{B = -A convolve[A, k]},
   MorphologicalComponents[ColorNegate[Binarize[Image[B], 3]]]]
```

```
m[A_] := Total[Total[A]] / Exp[Total[Log[Dimensions[A]]]]
```

```
cond := With[{t = Tally[Flatten[iθ[σ]]]},
   ! (Length[t] > 1 && SortBy[t, Last][[-1, +1]] == 0 &&
      Max[DeleteCases[t, _?(#[[1]] == 0 &)][[All, 2]]] ≤ 50)]
```

```
fv1 = {{-1, 0, +1}, {-1, 0, +1}, {-1, 0, +1}};
fv2 = {{0, 1, 0}, {0, 0, 0}, {0, 1, 0}};

fh1 = {{-1, -1, -1}, {0, 0, 0}, {+1, +1, +1}};
fh2 = {{0, 0, 0}, {1, 0, 1}, {0, 0, 0}};

ω[A_] := With[{B = (Abs[convolve[A, fv1]] - A convolve[A, fv2]),
   C = (Abs[convolve[A, fh1]] - A convolve[A, fh2])}, B + C]
```

Algorithm

```
σ = Array[-1 &, {250, 250}]; n = 1;
z := RandomReal[{0, 1}, Dimensions[σ]];

Monitor[While[True, σ = Sign[p[σ] - z]; n++;], n];
```

```
2 |
```

```
Dynamic[
 Refresh[MatrixPlot[σ, ImageSize → Medium, ColorRules → {-1 → White, +1 → Black}]],
 TrackedSymbols → {}, UpdateInterval → 1]
```

References

[1] Bovier, A. (2006). Metastability: A potential theoretic approach. In *ICM Proceedings*, pages 499–518.

[2] Bovier, A. (2009). Metastability. In *Methods of Contemporary Mathematical Statistical Physics*. Springer.

[3] Bovier, A. and Hollander, den, F. (2015). *Metastability: A Potential-Theoretic Approach*. Springer.

[4] Bovier, A., Hollander, den, F., and Nardi, F. (2006). Sharp asymptotics for kawasaki dynamics on a finite box with open boundary. *Probab. Theory Relat. Fields*, (135):265–310.

[5] Cirillo, E., Nardi, F., and Spitoni, C. (2008a). Competitive nucleation in reversible probabilistic cellular automata. *Phys. Rev.*, 78(040601).

[6] Cirillo, E., Spitoni, C., and Nardi, F. (2008b). Metastability for reversible probabilistic cellular automata with self-interaction. *J. Stat. Phys.*, 132(3):431–471.

[7] Cirillo, E. N. M. and Nardi, F. R. (2003). Metastability for a stochastic dynamics with a parallel heat bath updating rule. *J. Stat. Phys.*, 110(1):183–217.

[8] Derrida, B. (1990). Dynamical phase transitions in spin models and automata. In van Beijeren, H., editor, *Fundamental Problems in Statistical Mechanics*, volume VII, pages 273–309. Elsevier.

[9] Gaudillière, A. (2008). Condenser physics applied to markov chains: A brief introduction to potential theory. arXiv:0901.3053.

[10] Nardi, F. and Spitoni, C. (2012). Sharp asymptotics for stochastic dynamics with parallel updating rule. *J. Stat. Phys.*, 146(4):701–718.

[11] Sericola, B. (2013). *Markov Chains: Theory and Applications*. Wiley.